Title: Continental-Scale Carbonate Sedimentation and Environmental Correlates of the Shuram-Wonoka Excursion

Authors: *Daniel C. Segessenman[1,2] and Shanan E. Peters[2]

Affiliations:
1) Atmospheric, Oceanic, and Earth Sciences Department, George Mason University, Fairfax, Virginia, 22030, USA
2) Department of Geoscience, University of Wisconsin-Madison, Madison, Wisconsin, 53715, USA
*Corresponding Author: dsegesse@gmu.edu

Abstract

Strata of the Ediacaran Period record many Earth-Life features that distinguish the Neoproterozoic-Phanerozoic transition. However, it is difficult to determine cause and effect relationships between Ediacaran events. Continental-scale patterns of sedimentation have been used as proxies to investigate controls on Phanerozoic macroevolution, including sea level drivers and potential carbon cycling perturbations. Here we focus on quantitative properties of carbonate rock area, volume, geochemistry, and depositional environments from the North American Ediacaran System. Patterns of carbonate sedimentation and geochemistry are broadly coincident with transgressive/regressive cycles which have been linked to glacioeustacy and global/regional tectonics. Highly negative carbonate carbon isotope values distinguishing the Shuram-Wonoka carbon isotope excursion (SW-CIE) coincide with a distinct increase in carbonate quantity, which spans nearshore, outer shelf, and slope/basin depositional environments. An increase in the extent of carbonate sedimentation on the continent may indicate global marine transgression, suggesting that the excursion occurred during an interglacial warm period. This same increase in carbonate sedimentation is also broadly coincident with first occurrences of the Ediacaran biota. A subsequent increase in carbonate rock quantity in the latest Ediacaran, dominantly deposited in nearshore environments, coincides with the appearance of biomineralizers, potentially indicating common cause drivers for the extent of shallow shelves, carbonate sedimentation on the continents, and macroevolution. This analysis provides a robust, rock record-based chronostratigraphic framework within which major Ediacaran events can be anchored, new evidence of environmental correlates for several key features of the Ediacaran and provides a foundation for future hypothesis testing during the dawn of animal life.

1. Introduction

The Ediacaran Period is a critical transition in Earth's geological history, as reflected in its position as a boundary interval between the Proterozoic and Phanerozoic eons. The Ediacaran directly follows deglaciation of the global Cryogenian Snowball Earth glaciations; the last glaciations of great enough magnitude to cover all continents in ice sheets (Hoffman et al., 1998; Knoll et al., 2006; Hoffman and Li, 2009; Hoffman et al., 2017; Xiao and Narbonne, 2020). Ediacaran strata have been interpreted as having glacial influences, perhaps representing multiple episodes of glaciation in the mid-to-late Ediacaran (Hoffman and Li, 2009; McGee et al., 2013; Pu et al., 2016; Wang R. et al., 2023a; Wang R. et al., 2023b; Wang R. et al., 2023c; Kirshchvink, 2023; Fitzgerald et al., 2024; Wu et al., 2024). The oldest known complex macroscopic fossils that include some of the earliest metazoans, colloquially known as the Ediacaran biota, are found in mid-Ediacaran strata (Bobrovskiy et al., 2018; Xiao and Narbonne, 2020; Mussini and Dunn, 2023). The greatest magnitude negative carbon isotope ($\delta^{13}C$) excursion measured from the geologic record, known as the Shuram-Wonoka carbon isotope excursion (SW-CIE), has been identified globally from mid-Ediacaran carbonates (Burns and Matter, 1993; Grotzinger et al., 2011; Rooney et al., 2020; Xiao and Narbonne, 2020). The Ediacaran also marks the beginning of the end of the Great Unconformity, wherein there is a major increase from the latest Ediacaran to the mid-Cambrian in the quantity of preserved marine sedimentary rock in North America that was deposited on a diverse array of older Precambrian rock of many different types (Shahkarami et al., 2020; Peters et al., 2022; Segessenman and Peters, 2023; McDannell et al., 2022; Tasistro-Hart and Macdonald, 2023). Finally, the Ediacaran witnessed the final stages of the rifting of the supercontinent Rodinia, in addition to the amalgamation of Gondwana, a major transition in the Wilson supercontinent cycle (Wilson, 1966; Dewey and Spall, 1975; Schmitt et al., 2018; Condie et al., 2021; Ernst et al., 2021; Youbi et al., 2021; Nance, 2022; Macdonald et al., 2023; Müller et al., 2024). Directly following the Ediacaran and the disappearance of the Ediacaran biota, the uniquely 'explosive' Cambrian radiation of life occurs, which has its roots in latest Ediacaran evolutionary developments (Wood et al., 2019; Darroch et al., 2021; Servais et al., 2023; Segessenman and Peters, 2024). The oldest complex macroscopic fossils and high magnitude carbon isotope excursion identified from Ediacaran-age rocks globally have drawn increasing attention, both due to the appeal of working on the puzzles of extreme events and as an interval in Earth history that may be particularly informative for determining what planetary features may be important to the development of complex, macroscopic life prevalent on Earth today.

For all these reasons, the Ediacaran is a remarkable transition period in Earth history, but relatively low preserved rock quantity in comparison to the early Paleozoic (Segessenman and Peters, 2023; Bowyer et al., 2024) and a dearth of suitable index fossils for biostratigraphy makes correlating Ediacaran strata difficult (Xiao and Narbonne, 2020). New geochronologic constraints (e.g., Cantine et al., 2024; Tan et al., 2024) are being discovered and new methods for correlation (e.g. Hagen and Creveling, 2024) are being developed that seek to improve age models and our understanding of Earth systems evolution during the Ediacaran. Although studies like these are fundamental to improving our understanding of the Ediacaran, most of these approaches target key stratigraphic intervals regionally or globally and thus do not provide a full accounting of the period's complete rock record. Another approach that seeks to integrate all available stratigraphic data for a given interval in order to quantify the geologic framework and provide additional constraints on the nature of sampling and changes in the Earth system is macrostratigraphy (Peters, 2006; Peters and Husson, 2018; Peters et al., 2018; Peters et al., 2022;

Segessenman and Peters, 2023; Quinn et al., 2024). This approach has enabled quantitative analyses of continental sedimentation patterns and their geodynamic drivers (e.g., Phanerozoic Sloss sequences; Tasistro-Hart and Macdonald, 2023), analysis of relationships between igneous rock area and detrital zircon ages (Peters et al., 2021), examinations of correlations between rock quantity and biodiversity (e.g., Peters and Heim, 2011; Husson and Peters, 2017; Zaffos et al., 2017), and more (Peters et al., 2022). Of the rock types examined, macrostratigraphic quantities of carbonate have been identified as particularly useful for analyzing drivers of continental scale stratigraphic patterns.

Macrostratigraphic changes in carbonate quantity have been used as a proxy for continental flooding and to help constrain how Earth-life systems co-evolve (Valentine and Moores, 1970; Wilkinson and Walker, 1989; Peters, 2006; Peters, 2008; Hannisdal and Peters, 2011; Segessenman and Peters, 2023; Boulila et al., 2023; Alcott et al., 2024). Recently, stratigraphic data was compiled and developed for an Ediacaran-centric ‘mesostratigraphic’ framework, a focused macrostratigraphic approach in which only Ediacaran-age strata and rocks chronostratigraphically above and below were compiled from across North America, Central America, Greenland, and Svalbard (Segessenman and Peters, 2023). This analysis yielded additional perspectives on rock quantity and demonstrated that Ediacaran events are anchored within a shifting rock record that is responding to changes in the Earth system. For example, increases and decreases in the quantity and proportion of carbonates in the Ediacaran suggested a potential Sloss sequence-like cycle in the Ediacaran, which coincided with the SW-CIE (Segessenman and Peters, 2023) and biodiversity patterns (Segessenman and Peters, 2024). A previous depositional environment analysis of key Ediacaran carbonate sections globally found that the SW-CIE coincided with global transgression (Busch et al., 2022) and these authors concluded that the SW-CIE may have been a shallow marine focused result of enhanced primary productivity and/or evaporative processes that decoupled carbonate environments from global oceanic dissolved inorganic carbon (DIC).

There are numerous studies that propose mechanisms that do not require shifts in oceanic DIC to produce the globally occurring, extremely negative $\delta^{13}C$ values that are the signature of the SW-CIE in Ediacaran carbonates (e.g., Grotzinger et al., 2011; Schrag et al., 2013; Shields et al., 2019; Husson et al., 2020; Laakso and Schrag, 2020; Li et al., 2020; Xu et al., 2021; Busch et al., 2022; Cui et al., 2022; Shi et al., 2023; Wang W. et al., 2023). This is largely due to the SW-CIE reaching values far lower than the assumed -5‰ of volcanic CO_2 input and the SW-CIE's apparent multi-million year duration (Rooney et al., 2020; Cantine et al., 2024; Hagen and Creveling, 2024) which greatly exceeds the residence time of carbon in Earth's oceans (~0.1 m.y.) and breaks the carbon isotope mass balance of standard global carbon cycling models (Kump and Arthur, 1999; Busch et al., 2022). However, carbon cycling perturbation of oceanic DIC and mechanisms that could have decoupled shallow marine carbonate $\delta^{13}C$ need not be mutually exclusive. Geologic evidence for Laurentian rifting and a pulse of the Central Iapetus Magmatic Province (CIMP) coincides with the currently constrained interval for the SW-CIE (Condie et al., 2021; Youbi et al., 2021; Macdonald et al., 2023). The SW-CIE is stratigraphically bracketed by glacially influenced sedimentary rocks of the Gaskiers (below) and Luoquan/Hankalchough (above), suggesting a potential connection to climate and/or glacioeustacy (Wang R. et al., 2023b; Wang R. et al., 2023c; Fitzgerald et al., 2024; Wu et al., 2024). Assembly of the supercontinent Gondwana begins in the latest Cryogenian and reaches peak preserved orogen length during the mid-to-late Ediacaran (Meert and Lieberman, 2008; Ganade de Araujo et al., 2014; Oriolo et al., 2017; Schmitt et al., 2018; Condie et al., 2021;

Murphy et al., 2024). Large Igneous Province (LIP) emplacement, supercontinent assembly and breakup, and glaciations are mechanisms that have all been tied to Phanerozoic perturbations in oceanic DIC $\delta^{13}C$ and macroevolution (e.g., Kump and Arthur, 1999; Isson et al., 2019; Cramer and Jarvis, 2020; Condie et al., 2021; Green et al., 2022; Tian and Buck, 2022; Boulila et al., 2023).

Globally effective tectonic mechanisms known to have contributed to carbon cycling perturbation in Earth's past appear to have been active during the Ediacaran, but questions of specifically when they were active and the significance of their contribution to global environmental change remain. Here we present an updated mesostratigraphic compilation and analysis of Ediacaran carbonate quantity, depositional environments, and geochemistry from across the North American continent. The goal is to provide a comprehensive, quantitative dataset on Ediacaran stratigraphy, as currently represented in the published literature, that can be updated and adjusted as future research expands our understanding. Although this compilation and analysis cannot overcome the long-standing challenges of geochronology in the latest Neoproterozoic, it does provide a rock-based chronostratigraphic framework from which we can anchor evidence of significant Ediacaran events and potentially provide new perspectives on Earth systems evolution at the dawn of complex macroscopic life.

2. Methods

Bounding ages, thicknesses, lithologies, and proportional positions of 5,559 carbon isotope measurements within 548 Ediacaran age rock units were derived from the 'mesostrat' dataset of Segessenman and Peters (2023), with an additional 3,403 carbon isotopes compiled from multiple sources for this study. See Supplementary Table S1 and S2 for all compiled carbon isotope measurement data, including measured values, stratigraphic positions, references, and locations. Carbon isotope measurements were assigned ages based on their relative stratigraphic position within an age model that was constructed for the Ediacaran System in NA (for a complete description of the age model construction, see pages 401-404 of Segessenman and Peters, 2023). Construction of the age model involved assigning each rock unit a chronostratigraphic bin based on the published literature and then interpolating all unit boundary positions within that chronostratigraphic bin using super-positional constraints. This step was then followed by adjustments based on available radioisotopic data and regional correlations. Carbon isotope measurements were not directly used to construct the age model, though published age interpretations have been influenced by chemostratigraphic correlations. Several adjustments to Ediacaran rock unit bounding ages from Segessenman and Peters (2023) were made here to incorporate updates from studies published after the completion of the original mesostrat dataset (e.g., Busch et al., 2023; Ineson et al., 2024).

Carbonate-bearing stratigraphic units and associated $\delta^{13}C$ and $\delta^{18}O$ measurements were assigned to one of three marine depositional environments based on available interpretations (largely associated with interpreted depths of carbonate environments) in the literature: 1) shoreface to shallow shelf (nearshore); 2) non-nearshore continental shelf (outer shelf); and 3) continental slope to basin settings (slope/basin). This approach is similar to the environmental analysis of Busch et al. (2022), though with a coarser resolution encompassing all Ediacaran-age rocks across North America. A full list of Ediacaran carbonate bearing rock units, their associated environmental interpretation, and the primary reference for depositional environment interpretations is shown in Table 1. If no depositional environment interpretation was available in the literature, carbonate units were assigned to a general ‘inferred marine’ category. The primary carbonate phase (dolomite/calcite) of each measured isotope value was included when available. All compiled $\delta^{13}C$ and $\delta^{18}O$ data used for this study are included in the supplement (Table S1).

From the updated dataset of Ediacaran rocks, compiled carbon and oxygen isotope measurements, depositional environment interpretations, and quantities of rock were expressed as a time series. Area and volume flux (sum of thickness times column area divided by rock unit duration) were the primary quantities calculated as time series and were divided into categories of: 1) carbonate depositional environments (as listed above), 2) total carbonates, 3) total siliciclastics, 4) dolostone only, and 5) limestone only. Rock units with multiple lithologies were split into lithologic categories based on the relative proportion of each lithology recorded for that rock unit. All rock quantity values have a 3 m.y. smoothing applied, which is on the order of the expected minimum error in the age model. Raw carbon isotope values, categorized by depositional environment and phase, were then plotted with the calculated rock quantities, using the same integrated age model. Next, 5 m.y. moving window averages (with 3 m.y. smoothing) of carbon and oxygen isotope values were calculated by locality, phase, and depositional environment. For each moving window average of carbon and oxygen isotopes, an average value for each locality was calculated first to avoid overweighting localities with higher numbers of samples. Correlations between $\delta^{13}C$ and $\delta^{18}O$ values, categorized by depositional environment, were calculated using Spearman's ρ with a 5 m.y. moving window. 2 standard deviation error bars and envelopes were calculated for carbon/oxygen isotope averages and the $\delta^{13}C/\delta^{18}O$ correlations using block bootstrap resampling. Overlays highlighting potentially relevant Ediacaran Period events (e.g. Gaskiers glaciation, advent of calcifying taxa, etc.) were added to each of the time series with timings based on current interpretations in the published literature.

3. Results

Ediacaran rock-bearing column areas (shown as polygons) in North America, Greenland, and Svalbard, with those bearing carbonates and geochemical analyses highlighted, are shown in Figure 1. The Ediacaran record of North America is limited to the highly deformed remnants of the ancient margins of Laurentia, except for terranes in SE Canada and NW United States that are interpreted as either peri-Gondwanan or peri-Baltican volcanic arcs accreted to Laurentia during the Paleozoic (Beranek et al., 2023; Murphy et al., 2023; Keppie and Keppie, 2024). The majority of North America's Ediacaran age carbonate rock is found along its western margin, and, consequently, most geochemical analyses are also found in those regions (NW Canada, SW U.S.A., and NW Mexico). The locations, primary references, approximate stratigraphic positions, and reported values of geochemical analyses used for this study are available in the supplementary information associated with this study (Supplementary Tables S1-2).

North American Ediacaran carbonate area and volume exhibit similar trends and are largely interchangeable metrics for rock quantity in this study. Ediacaran carbonate quantity starts off relatively high in the earliest Ediacaran, particularly among shallow environments, a feature indicative of post-Marinoan deglaciation and cap carbonate deposition (Figure 2A-B). Carbonate quantity drops off sharply post cap carbonate deposition and remains low in all environments until a stepwise increase at ~590 Ma. Between 585-580 Ma there is sharp increase in carbonate quantity of all environments, but particularly in the slope/basin, that culminates in the greatest area and volume flux of Ediacaran carbonate, between 580 and 570 Ma. Following this maximum, there is a sharp decrease to a local minimum by 565 Ma. Another sharp increase and decrease in carbonate quantity occurs between 562 and 555 Ma, before another sharp decrease between 555 and 550 Ma. The second increase is largely driven by slope/basin environments for volume flux and among shelf carbonates for area. This is followed by a final increase in carbonate quantity, driven primarily by shallow carbonates between 550 and 545 Ma, which then sharply decrease to pre-590 Ma values during the terminal Ediacaran (Figure 2A-B). Carbonates represent the greatest proportion of total sedimentary rock quantity during the deposition of cap carbonate in the earliest Ediacaran and during the 580-570 carbonate quantity maximum (Figure 2A-D).

Carbon isotope values ($\delta^{13}C$) associated with cap carbonate deposition during the earliest Ediacaran are highly variable, ranging from ~8‰ to as low as -11‰ (Figure 1A). Between 620 Ma and 595 Ma there are relatively few carbon isotope measurements available, due in part to the decreased quantity of carbonates (and sedimentary rock in general) during this interval. A highly negative cluster of slope/basin carbon isotope values at 610-600 Ma are from carbonates of the Geikie Siding Mbr of the Old Point Fort Fm, which has a date of 607.8 ± 4.7 Ma (Kendall et al., 2004; Cochrane et al., 2019). At ~595 Ma, carbon isotope measurements become more abundant, coincident with the initial stepwise increase of carbonate quantity (Figure 1A). From 595-575 Ma, carbon isotope values in all three environment categories exhibit significance variance but steadily increase values as high as +11‰, before precipitously decreasing to values as low as -16‰; this shift is coincident with the carbonate volume and area maximum observed from 580-565 Ma (Figure 1A). From the excursion nadir at ~572 Ma, carbon isotope values climb to values ranging between about +4‰ and -4‰. The climbing positive values, sharp decrease to extremely negative values, and subsequent increase to more positive/stable values between 585 and 565 Ma is the signature of the SW-CIE. The excursion is bracketed by hypothesized glaciations of the Gaskiers and the Luoquan/Hankalchough, coincident with an episode of higher activity Laurentian rifting, positioned within the proposed timeframe for the Ediacaran ultraweak magnetic field event (Bono et al., 2019; Domeier et al., 2023; Huang et al., 2024), and coincides with the appearance of the oldest complex macroscopic fossils of the Ediacaran biota (Figure 1A). Carbon isotope values hold relatively steady for the remainder of the Ediacaran, although with an overall decreasing trend and a possible negative excursion (only from shallow marine carbonates) at 550-545 Ma that coincides with the second and final carbonate quantity increase and the advent of Ediacaran calcifying taxa (Figure 1A).

Carbonate rock quantities, separated by their dominant carbonate type (dolostone or limestone), exhibit departures from the aggregate carbonate record (Figure 3A-E). Limestone is rare to non-existent from the earliest Ediacaran to 590 Ma (Figure 3B,D). Shallow marine dolostone makes up the majority of this early record, including that of the cap carbonate (Figure 3C,E). Both limestone and dolostone quantities increase at ~585 Ma, though dolostone quantities are more pronounced between 580 and 565 Ma. Slope/basin carbonates are the largest contributor to the volume flux of both limestone and dolostone within the Shuram-Wonoka interval. Dolostone associated with all three environmental categories makes up the largest proportion of carbonate area within the Shuram-Wonoka interval. The second pulse of carbonate volume flux from 565-555 Ma is dominated by limestone and slope/basin environments. The final pulse of carbonate quantity from 550-545 Ma is evenly distributed between dolostone and limestone, predominately deposited in shallow marine environments.

Averaged Ediacaran carbon isotope values separated by locality, phase, and environment largely follow the overall trends observed in the aggregate values, though there are some differences. Average carbon isotope values are between 0 and -4‰ during the earliest Ediacaran and remain relatively steady until around 620 Ma, when error increases and averaged carbon isotope values fluctuate due to the paucity of carbonate-bearing units (Figure 4A-C). At ~595 Ma, values stabilize as the number of localities with carbonate increases and exhibit increasingly positive values before the precipitous decrease to the very negative values (<-6‰) that define the SW-CIE between 580 and 565 Ma. Carbon isotope values increase to around 0‰ by ~565 Ma and then show a slight downward trend for the rest of the Ediacaran, with a potential negative excursion after 545 Ma (Figure 4A-C).

Carbon isotope values averaged by locality exhibit similar overall trends, but with differing magnitudes. Some localities do have anomalously high values in the Shuram interval (Virginia and SW Canada), though the sections bearing these measurements also have greater stratigraphic and positional uncertainties within the age model (Figure 4A). Averages of carbon isotopes separated by reported carbonate phases follow the same general trends, but dolomite averages do not reach positive values (+6‰ maximum) as great as those of calcite (+9‰ maximum). Calcite values also appear to be more negative than dolomite within the Shuram-Wonoka interval (-9‰ for calcite vs. -6‰ for dolomite). Thus, the magnitude of the paired positive-negative excursion of the Shuram-Wonoka is typically more attenuated in dolomite samples (Figure 4B). Carbon isotope values averaged by environmental categories exhibit similar overall trends, though the slope/basin setting appears to have a delayed positive increase compared with nearshore and middle/outer shelf samples (Figure 4C). Averaged values of all three environmental categories reach similarly negative values within the Shuram-Wonoka interval (-7‰ minimum), suggesting a ubiquitous shift across carbonate depositional environments (Figure 4C).

Correlations between $\delta^{13}C$ and $\delta^{18}O$ in all three environmental categories exhibit moderate ($\boldsymbol{\rho}$ >=0.5) to strong ($\boldsymbol{\rho}$ >= 0.75) positive correlation in the earliest Ediacaran. This correlation decreases but can't be calculated after 620 Ma due to insufficient data (Figure 4D). All environmental categories have sufficient data by 575 Ma, and all environmental categories exhibit increases in $\delta^{13}C$ and $\delta^{18}O$ correlations from weak/no ($\boldsymbol{\rho}$ = 0 to 0.25) to moderate and strong positive within the Shuram-Wonoka interval. Correlations fluctuate but generally decrease to weak ($\boldsymbol{\rho}$ <= -0.25) and moderate negative correlations ($\boldsymbol{\rho}$ <= -0.5) after 565 Ma and increase to weak positive correlations by the end of the Ediacaran (Figure 4D).

Carbonate oxygen isotope values ($\delta^{18}O$) were analyzed by environment, locality, and phase using the same methods applied to carbon isotope values (Figure 5). With some exceptions, Ediacaran carbonate $\delta^{18}O$ generally fluctuates within a range of 0 to -15‰. When separated by relative environmental category, nearshore carbonate $\delta^{18}O$ is generally more positive on average than the outer shelf or slope/basin settings, with the exceptions of the early Ediacaran (low data availability) and a sharp decrease at ~562 Ma near the onset of proposed Luoquan/Hankalchough glaciation onset (Figure 5B). Interestingly, nearshore $\delta^{18}O$ values exhibit a similar trend to their $\delta^{13}C$ counterparts within the SW-CIE (climb to more positive values pre-Shuram, extended decrease within Shuram, post-Shuram rise to more positive values), while outer shelf and slope/basin values vary less and do not follow this trend (Figures 4C; 5B). As might be expected, $\delta^{18}O$ varies between localities, though a couple of features stand out: 1) NW Canada, Death Valley, and Svalbard localities show relatively greater agreement in the earliest Ediacaran than at any other time in the Ediacaran, and 2) the nearshore Shuram-Wonoka trend in $\delta^{18}O$ mainly mirrors that of the Death Valley region (Figure 5C). $\delta^{18}O$ averaged by carbonate phase (calcite and dolomite) are relatively stable, follow similar trends, but exhibit distinct values during the early Ediacaran (Figure 5D); dolomite is consistently more positive by ~3‰ during intervals with greater amounts of data. Both phases then track similarly through the low data interval, with a significant decrease largely reflecting trends from SW Canada (Figure 5D). Both phases have a Shuram-like trend coincident with that of $\delta^{13}C$ (~580-565 Ma), however, calcite has a greater magnitude decrease immediately before the Shuram that coincides with the Gaskiers glaciation and the Shuram-like excursions of dolomite and calcite are offset temporally. After the Shuram, calcite and dolomite average values separate as in the early Ediacaran (dolomite more positive than calcite) but both phases fluctuate more, with calcite in particular exhibiting larger fluctuation between -9‰ and -18‰ (Figure 5D).

4. Discussion

The Ediacaran System is uniquely positioned as a transition interval between a protracted period of rather low preserved sediment quantity and markedly higher sediment abundance starting in the Cambrian, a prominent transition in the rock record marked in many places by the Great Unconformity (Peters et al., 2018; Shahkarami et al., 2020; Ma et al., 2022; McDannell et al., 2022; Segessenman and Peters, 2023, Tasistro-Hart and Macdonald, 2023). The ancient Laurentian margins on which Ediacaran sedimentary rocks were deposited have been deformed and dissected by a variety of distinct tectonic events (e.g., Ma et al., 2023; Macdonald et al., 2023; van Staal and Zagorevski, 2023; Weil and Yonkee, 2023). The North American Ediacaran record (particularly that of the east coast) is also a composite record of ancient Laurentian continental margins and accreted peri-Gondwanan or peri-Baltican volcanic arc terranes (Beranek et al., 2023; Murphy et al., 2023; Keppie and Keppie, 2024). Existing geochronologic constraints for Ediacaran stratigraphy are limited (relative to the Phanerozoic), not due to a lack of effort, but due to generally limited availability of accessible Ediacaran outcrop, conventionally dateable material, and traditional biostratigraphic controls (Xiao and Narbonne, 2020).

As an additional challenge, all Ediacaran sedimentary rocks have experienced some degree of diagenesis and/or tectonic deformation, and many latest Neoproterozoic age rocks, particularly those from the SE United States, are well categorized as metasedimentary (e.g., Thomas, 1991; Hatcher, 2010; Waldron et al., 2019). Nevertheless, a wide range of studies have made considerable progress towards understanding these rocks (e.g., Canfield et al., 2020; Rooney et al., 2020, Busch et al., 2022; Bowyer et al., 2024; Cantine et al., 2024; Wei et al., 2024). The North American compilation of Ediacaran stratigraphy used here (Segessenman and Peters, 2023) was constructed with the intent to represent the aggregated Ediacaran system as it stands in the published literature. Marine carbonate quantity, presence/absence, and geochemistry have all been interpreted as reflecting various local and global-scale geologic processes during the Phanerozoic (e.g., Ahm and Husson, 2022; Peters et al., 2022; Segessenman and Peters, 2023; Hohmann et al., 2024), and we apply that same general methodology here. Our compilation generally agrees with other published summaries (e.g., Fig. 2 of Macdonald et al., 2023; Bowyer et al., 2024; Cantine et al., 2024), although we acknowledge that our understanding of all rocks everywhere is subject to change as new studies of them unfold.

4.1 Geologic Context of Ediacaran System Carbonates

A recent study that simulated carbonate records to determine how preservation affected interpretations of macroevolution by Hohmann et al. (2024) found that rarer, prolonged unconformities were more influential than the degree of stratigraphic completeness on recovering and interpreting ‘true’ macroevolutionary trends. They concluded that stratigraphic sections that are incomplete but have more regular hiatus frequency/duration enable recovery of macroevolutionary trends and that understanding processes that can influence stratigraphic architecture are critical for interpretation of macroevolution. This suggests that it is possible for process signals to be recovered from the aggregated Ediacaran stratigraphic record despite its decreased preservation relative to the Phanerozoic. Based on current correlations of the Ediacaran across Laurentia, periods of widespread hiatuses within the sections where the Ediacaran is preserved are between ca. 600-590 Ma, ca. 562-555 Ma, and across the Ediacaran-Cambrian boundary (see Figure 2 in Macdonald et al., 2023; Segessenman and Peters, 2023; Bowyer et al., 2024). Furthermore, the nature of the Ediacaran's upper boundary with the Cambrian suggests a relatively narrow timeframe for potential focused erosion of Ediacaran strata during the Phanerozoic.

Although there is a globally recognized hiatus commonly present at the Ediacaran-Cambrian boundary (Shahkarami et al., 2020; Bowyer et al., 2022; Bowyer et al., 2024), Ediacaran sedimentary sequences are generally overlain by Cambrian marine sediments (Segessenman and Peters, 2023; Bowyer et al., 2024). It is rare that an Ediacaran sedimentary sequence is overlain by sedimentary sequences younger than Cambrian, in that essentially everywhere Ediacaran age sedimentary rocks are preserved, they were sealed by the deposition of Cambrian sedimentary rocks across the Ediacaran-Cambrian transition. This observed relationship between the Ediacaran and Cambrian Systems suggests that the decreased quantity of preserved rock in the Ediacaran (relative to the following Paleozoic; Segessenman and Peters, 2023) is less a signal of erosion of a formerly much more extensive Ediacaran sedimentary rock record, but is instead an indication of limited accommodation and lack of sedimentation on the continents to begin with. The proportion of the preserved sedimentary record that is carbonate (Fig. 2), which is primarily driven by base-level associated accommodation on continental margins (Miall, 2016), reinforces this view. We interpret this as an indication that the changes in

North American Ediacaran carbonate quantity are representative primarily of 2nd order (10^7 yr) to 3rd order (10^6 yr) scale changes in epicontinental marine deposition reflecting a combination of local and global geologic processes.

4.2 Cap Carbonate Deposition

The base of the Ediacaran is marked by the appearance of a global cap carbonate that represents deglaciation at the end of the Cryogenian snowball Earth episodes (Hoffman et al., 1998; Knoll et al., 2006). Models suggest a rapid transition from snowball Earth conditions in the latest Cryogenian to a 'supergreenhouse' state as volcanically sourced atmospheric CO_2 exceeded the threshold to initiate global glacial retreat and resulted in rapid transgression on continental margins (Creveling and Mitrovica, 2014; Myrow et al., 2018). The extreme hothouse conditions are thought to have led to an oversaturation of CO_2 in the ocean-atmosphere system, ultimately leading to the deposition of the distinctive cap carbonate that marks the base of the Ediacaran (Sun et al., 2022). Cap carbonate deposition on Laurentia can be recognized by the elevated quantity of carbonate rock (dominantly dolostone; Fig. 3B-E) preserved in the earliest Ediacaran and that the earliest Ediacaran record has the greatest proportion (nearly 50%) of sedimentary rock units that contain carbonate (Figs. 2, 3). While the proportion of the Ediacaran marine sedimentary record that contains carbonate decreases throughout the Ediacaran, cap carbonate sequences do not represent the greatest Ediacaran quantity of carbonate material in Laurentia, a result that is contrary to what might be expected (Fig. 2).

Sections that definitively preserve the earliest Ediacaran on North America are rare, even when considering the Ediacaran's overall decreased preserved rock quantity. Carbonate quantity in the earliest Ediacaran of Laurentia is largely represented by the Noonday Dolomite in the SW contiguous USA, the Hayhook and Ravensthroat formations from NW Canada, the Katakturuk Dolomite from NE Alaska, the base of the Dracoisen Formation in Svalbard, and the Canyon Formation from East Greenland. With the exceptions of the Katakturuk and Noonday Dolomite formations, cap carbonate formations of North America are thin, generally <20m thick (Fairchild and Hambrey, 1995; Macdonald et al., 2009; Macdonald et al., 2013; Creveling et al., 2016). Despite representing the highest proportion of the sedimentary record that contains carbonate at any time in the Ediacaran, the relative rarity and generally short-lived stratigraphic expression of the Ediacaran cap carbonate in North America explains why its estimated area and volume are eclipsed by that of the mid-Ediacaran Shuram interval, in which the frequency of carbonate bearing sections increases across a higher number of stratigraphic sections with larger areas and greater thicknesses (Fig. 2C-D).

Based on projections of the terminal Cryogenian deglaciation's effect on sea level (Creveling and Mitrovica, 2014; Myrow et al., 2018), it is not particularly surprising that the carbonate area and volume increases in the earliest Ediacaran are largely associated with nearshore environments, though isotopic sampling captures all three environmental categories in the earliest Ediacaran on North America (Figs. 2-5). The dominance of dolostone and strong to moderate positive correlations ($\rho >= 0.75$ and 0.5 respectively) between $\delta^{13}C$ and $\delta^{18}O$ from all environmental categories (Figs. 3E,4D) in the earliest Ediacaran suggests potential diagenetic influences and/or increased ocean alkalinity, which is consistent with high resolution global geochemical analyses and interpretations of the earliest Ediacaran cap carbonate (Hoffman, 2011; Ahm et al., 2019; Sun et al., 2022). High variance of raw carbon isotope values (+8 to -7‰) during the earliest Ediacaran is another well documented observation attributed to local diagenetic effects (Ahm et al., 2019), although average $\delta^{13}C$ values categorized by phase and by environment remain strikingly close (within 1-2‰) of each other before diverging and exhibiting more variance for the rest of the Ediacaran (Fig. 2B-C). In contrast, $\delta^{18}O$ values are distinctly separate when categorized by phase and environment in the earliest Ediacaran (Fig. 5B,D), exhibiting the mass balance modeled expectation of an ~3‰ difference between the calcite and dolomite phases (Land, 1980; Swart, 2015). These results are consistent with globally observed and analyzed features from the earliest Ediacaran, including the estimated proportion of the sedimentary record that is carbonate. The intriguing result here is that the carbonate proportion is at a maximum in the earliest Ediacaran and continuously declines (with fluctuations) throughout the remainder of the period, even though siliciclastic flux doesn't significantly increase until the mid-Ediacaran (Fig. 2C-D). This could reflect overall decreasing oceanic carbonate saturation throughout the Ediacaran as carbonates were deposited in the limited accommodation on continental margins and/or a general drowning of carbonate environments by increased siliciclastic input, with exceptions for pulses of increased carbonate preservation, such as during the SW-CIE (Fig. 2).

4.3 Early Ediacaran low preserved rock interval

The post-cap carbonate early Ediacaran sedimentary record from North America is sparsely represented (Figs. 2-5) by thicker, long-ranging rock units, such as the Sheepbed Fm from NW Canada, the undifferentiated lower Johnnie Fm of the SW USA, the Dracoisen Fm of Svalbard, the Morænesø Fm from northern Greenland, and the Canyon Fm from east Greenland (see references in Segessenman and Peters, 2023). This interval includes the lowest counts of distinct marine sedimentary units observed during the Ediacaran and low preserved rock volume/area (Fig. 2). Interestingly, the proportion of sedimentary rock that is carbonate fluctuates, but consistently decreases through this interval, as it appears to do for the entire Ediacaran Period (Fig. 2D). The low (and sometimes non-existent) amount of preserved carbonate and few geochronologic constraints explains the low number of isotopic analyses in this interval and the increase in the error envelope for isotopic averages (Figs. 4,5). The apparent excursion from ~610-600 Ma is due to isotopic measurements from the Old Fort Point Fm of SW Canada, which bears an early Ediacaran Re-Os date of 607.8 ± 4.7 Ma (Kendall et al., 2004; Cochrane et al., 2019). A lower Ediacaran (from cap carbonate to ~590 Ma) hiatus appears to be a common feature of the Ediacaran System on multiple continents, suggesting a potential global driver of low rock preservation during this interval (Cantine et al., 2024; Li et al., 2024). Despite the lack of data, the general absence of preserved rock during this often greater than 40 m.y. interval is interesting in and of itself and may indicate geologic processes that contributed to the lack of rock preserved from this time (Miall, 2016). More specifically, limited accommodation for sediments on continents (Segessenman and Peters, 2023), reverse weathering processes (Isson and Planavsky, 2018; Zheng et al., 2024) and outgassing from Laurentian rifting, and/or early pulses of CIMP magmatism (Ernst et al., 2021; Macdonald et al., 2023) could have maintained elevated $p\mathrm{CO_2}$ (and therefore a more erosive period) in a warm/hothouse following Marinoan deglaciation. Conversely, increasing orogenic activity (Schmitt et al., 2018; Condie et al., 2021; Müller et al., 2024) and associated $p\mathrm{CO_2}$ drawdown may have driven an overall cooler climate and decreased rates of erosion (outside of Gondwanan orogenic zones) during the early to middle Ediacaran (Fan et al., 2025).

4.4 Mid-Ediacaran rock quantity increase, Gaskiers glaciation, and the SW-CIE

The end of the low preserved rock interval, indicated by the rising limb of preserved siliciclastic and carbonate quantity at ~585 Ma, coincides with strata containing evidence of the Gaskiers glaciation (Fig. 2). The increase in preserved sediment quantity is opposite of what is generally expected during a glacial interval, but we attribute this rock quantity increase to Laurentian specific tectonic controls, such as continental margin subsidence and rift-associated accommodation (Busch et al., 2022; Segessenman and Peters, 2023). Evidence of glaciation in the Gaskiers Fm had been tightly constrained to a timeframe of ~340 kiloyears between 579.63 ± 0.15 and 579.88 ± 0.44 Ma (Pu et al., 2016). However, recent studies of the underlying Mall Bay Fm suggest a longer-term onset and duration for the Gaskiers glaciation (Fitzgerald et al., 2024). The overall geographic distribution and duration of globally occurring upper Ediacaran glacial intervals is an area of continuing research and geochronologic constraints that provide exact timings of Ediacaran strata interpreted as bearing glacial influences are rare, which allows for multiple models of mid-late Ediacaran glaciation (Kirschvink, 2023; Wang R. et al., 2023b; Wang R. et al., 2023c; Wu et al., 2024). Despite the difficulty in establishing a robust temporal framework, glacially influenced strata occur stratigraphically above and below carbonates bearing the highly negative $\delta^{13}C$ values of the SW-CIE, suggesting that there are glacial periods before and after the excursion, but as of yet, no definitive constraints have placed glaciation as coeval with the SW-CIE (Wang R. et al., 2023c, Fitzgerald et al., 2024, Wu et al., 2024). There do not appear to be any significant changes in $\delta^{13}C$ or carbonate quantity directly associated with the Gaskiers glaciation, although there are apparent negative excursions in outer shelf and slope/basin average $\delta^{18}O$ values that coincide with a positive $\delta^{18}O$ trend in the nearshore, which may suggest a response of carbonate $\delta^{18}O$ to glaciation/deglaciation during this interval (Figs. 2-5). $\delta^{18}O$ is thought to increase during glacial periods and decrease during deglaciation (Swart, 2015), so their coincidence may reflect age model inaccuracies. The $\delta^{18}O$ value of carbonates is also considered to be much more susceptible to diagenetic effects, so ultimately these apparent trends may be coincidental. While there do not appear to be clear trends in carbonate geochemistry or quantity associated with the Gaskiers glaciation, the proposed end of the Gaskiers does appear to be associated with the much more distinctive signals of the SW-CIE.

Carbonates bearing the SW-CIE were deposited within transgressive systems tracts globally (Busch et al., 2022) and analyses of global Ediacaran sedimentary rock quantities from key stratigraphic sections have suggested increased sedimentary rock accumulation rates and an increased flux of previously limited elements (e.g., sulfate and phosphorus) from terrestrial environments starting in the mid-Ediacaran (Cantine et al., 2020; Dodd et al., 2023; Segessenman et al., 2023; Walton et al., 2023; Wang H. et al., 2023; Bowyer et al., 2024; Cantine et al., 2024). Mid-Ediacaran carbonate area and volume increases in all environmental categories across Laurentia and compiled $\delta^{13}C$ measurements categorized by phase and depositional environment exhibit similarly negative trends for the SW-CIE (Figs. 2-4). The duration of the SW-CIE, assuming it is a synchronous signal, has been constrained to be on the order of 5 million years or less (Cantine et al., 2024; Hagen and Creveling, 2024). The length of the excursion, its direct coincidence with stratigraphic evidence suggesting a continental-scale flooding sequence (Busch et al., 2022; Segessenman and Peters, 2023; Bowyer et al., 2024; Segessenman and Peters, 2024), and its stratigraphic bracketing by glacially influenced strata suggests the possibility that the SW-CIE could represent an interval of warming between two intervals of glaciation, similar to that of the Trezona anomaly (albeit with potentially less extreme glaciation), which is measured from carbonates deposited after Sturtian deglaciation but before the Marinoan glaciation (Halverson et al., 2020; Ahm et al., 2021).

Many studies have provided hypotheses explaining the SW-CIE's extreme magnitude in ways that obviate the need for classic drivers (e.g., enhanced CO_2 outgassing) of major perturbations to the carbon cycle and oceanic DIC (e.g., Derry, 2010; Schrag et al., 2013; Lee et al., 2015; Cui et al., 2017; Shields et al., 2019; Cao et al., 2020; Cui et al., 2022; Wang H. et al., 2023; Gu et al., 2024) due to the potential for sampling bias in a geologic period with decreased rock preservation (Husson et al., 2020; Busch et al., 2022; Segessenman and Peters, 2023) and difficulties in applying Phanerozoic carbon cycling and isotope mass balance models (e.g., Kump and Arthur, 1999) to a seemingly multi-million year, high magnitude CIE (Grotzinger et al., 2011; Gong and Li, 2020; Rooney et al., 2020; Busch et al., 2022; Cantine et al., 2024; Hagen and Creveling, 2024; Tan et al., 2024). However, longstanding geologic evidence indicates that there are several global-scale geologic mechanisms operating in the latest Neoproterozoic that could be associated with carbon cycling perturbations (as recognized by others, e.g., Caxito et al., 2021; Cui et al., 2021; Youbi et al., 2021; Busch et al., 2022), including the final stages of Rodinia rifting and associated LIP emplacements of the Central Iapetus Magmatic Province (Youbi et al., 2021; Macdonald et al., 2023; Müller et al., 2024), initiation of the Gondwanan supercontinent amalgamation (Oriolo et al., 2017; Schmitt et al., 2018; Condie et al., 2021), and the Acraman mid-Ediacaran bolide impact crater (with estimated impact energy great enough to exceed theoretical global catastrophe threshold), which has been associated with turnover in Ediacaran primary producers (Williams and Schmidt, 2021; Figs. 2-5; Table 2). These potential mechanisms for carbon cycling perturbation need not be mutually exclusive with existing hypotheses explaining the extreme magnitude of the SW-CIE, but rather provide potential mechanisms for decreasing oceanic DIC $\delta^{13}C$ that could have been modified by factors unique to mid-Ediacaran oceans (e.g. enhanced organic matter oxidation, increased sulfate flux, microbial mediation, evaporation on shallow shelves etc.), leaving a global carbonate $\delta^{13}C$ signal that represents a complex mix of factors. Although post-burial diagenesis as a primary driver of SW-CIE $\delta^{13}C$ values (Derry, 2010) is now considered unlikely (e.g., Husson et al., 2020; Cui et al., 2021; Busch et al., 2022), increasing positive correlations between $\delta^{13}C$ and $\delta^{18}O$ values during the SW-CIE in all environmental categories may indicate the influence of ubiquitous in-situ and/or more immediate post depositional diagenetic effects (Fig. 4D). Increasingly positive correlations between $\delta^{13}C$ and $\delta^{18}O$ during the SW-CIE that then precipitously decrease during the recovery (Fig. 4D) could also be indicative of an increased flux of oceanic alkalinity (Spero et al., 1997) as a driver of increased carbonate deposition.

Although carbon cycling perturbation need not be mutually exclusive with existing hypotheses explaining the extreme magnitude of the SW-CIE, the results presented and discussed above suggest that explanations must also provide a mechanism for the coincident increase in carbonate quantity across depositional environments that had a dominantly dolostone phase (Figures 2, 3; Macdonald et al., 2023; Segessenman and Peters, 2023; Bowyer et al., 2024). The SW-CIE was coincident with the largest increase in dolostone quantity observed during the Ediacaran (post-cap carbonate), with subsequent carbonate quantity increases dominantly reported as limestone (Fig. 3). Until recently, this observation may have suggested diagenetic effects on SW-CIE carbonates due to the nature of the 'dolomite problem' in which there has been a long-standing challenge in understanding mechanisms of primary dolomite deposition (Land, 1998). Although there is still much to be understood about potential primary dolomite precipitation (Kim et al., 2023; Wang W. et al., 2023), it has recently been demonstrated that abiotic primary dolomite precipitation can occur when dissolved silica is present in high Mg:Ca ratio solutions at room temperature (Fang and Xu, 2022a; Fang and Xu, 2022b; Fang et al., 2023). Mid-Ediacaran bedded chert from North America has been reported in the Drook Fm (labeled as chemical sediments/evaporitic in Segessenman and Peters, 2023) of Newfoundland and coincides with the SW-CIE, a potential indicator of elevated dissolved silica in mid-Ediacaran oceans (Keppie et al., 1979; Williams and King, 1979; Segessenman and Peters, 2023). Furthermore, dissolved silica has been implicated as an influential factor for the soft-bodied Ediacaran biota's unique preservation within siliciclastic rocks (Tarhan et al., 2016; Slagter et al., 2021; Slagter et al., 2024), some of the oldest examples of which temporally overlap with the SW-CIE interval (Figs. 2-3; Table 2). This also coincides with increased Gondwana amalgamation orogenesis and felsic CIMP LIP emplacement (Aleinikoff et al. 1995; Southworth et al., 2009; Schmitt et al., 2018; Condie et al., 2021; Müller et al., 2024), a potential source for increased silica input to the mid-Ediacaran oceans (Figs. 2-5; Table 2). Siliciclastic weathering in a higher pCO_2 atmosphere can be a significant source of ocean alkalinity, a potential tie-in to the increased correlation between $\delta^{13}C$ and $\delta^{18}O$ during the SW-CIE (Fig. 4D; Halevy and Bachan, 2017; Middelburg et al., 2020) Considering these studies, the relative rarity of Ediacaran biota-style preservation in the Phanerozoic may be attributed to the radiation of biosilicifiers such as sponges and radiolarians drawing down oceanic dissolved silica during the early Cambrian (Conley et al., 2017; Ye et al., 2021). This may also help to explain the assumed (but still debated) decreased prevalence of dolomite through geologic time (Schomaker et al., 1985; Li et al., 2021; Husson and Coogan, 2023), potentially signifying Ediacaran dolomite quantity and Ediacaran biota preservation styles as additional factors that mark the Ediacaran as a critical transition period.

During the SW-CIE's 'recovery' interval to less negative $\delta^{13}C$ values, there is a sharp decrease in carbonate quantity that is immediately followed by another sharp carbonate quantity increase (dominantly limestone) that is not associated with a $\delta^{13}C$ excursion, which coincides with the timeframe of the proposed Luoquan glaciation (Figs. 2-5; Table 2). The bracketing of the SW-CIE by glacially influenced strata, like that of the Trezona anomaly (Halverson et al., 2020), may indicate that the SW-CIE took place during an interglacial warm/hot interval. The mechanisms that could have driven this potential relative model of mid-Ediacaran events have been laid out above: Gondwana amalgamation increases in orogenic belt length increased weathering induced CO_2 drawdown, which may have eventually induced glaciation (in addition to other factors that affect Earth's climate sensitivity, e.g., latitudinal distribution of continents) associated with the Gaskiers. The Acraman impact event appears unlikely to have been an initiator of the Gaskiers glaciation, as there is evidence of ice-rafted debris stratigraphically above and below the Acraman's associated ejecta band (Gostin et al., 2010; Williams and Schmidt, 2021). Depending on the extent of glaciation, ice coverage could have slowed the rate of weathering related CO_2 drawdown, and when paired with coeval CIMP LIP outgassing, tipped the climate threshold to a warm/hothouse state. During this warm interval, rates of weathering would have accelerated (including of the emplaced Catoctin LIP, which consists of felsic volcanics; Aleinikoff et al., 1999; Southworth et al., 2009) and delivered elevated rates of elements such as sulfur, phosphorus, and silica to the mid-Ediacaran oceans, which may have played an influential role in the SW-CIE, transient O_2 ventilation of the oceans, and the first occurrences of the Ediacaran biota and their unique taphonomy (Figs. 2-5). A transition from glaciation to a warm/hothouse state would have contributed to transgressive systems tracts associated with the SW-CIE, and a return to glacial conditions after the SW-CIE could explain the sharp decrease in carbonate quantity, although this could be caused by siliciclastic drowning of carbonates at this time as well. The Luoquan glaciation that follows the SW-CIE interval may represent the accelerated weathering drawdown of atmospheric CO_2 from continued Gondwana amalgamation and/or weathering of CIMP volcanics that initiated a return to cool/icehouse conditions, in a similar cycle as proposed for the Cryogenian return to Snowball Earth after Sturtian deglaciation (Hoffman and Schrag, 2002; Nance, 2022).

4.5 Carbonate environments, the Ediacaran biota, and the appearance of biomineralizers

Late Ediacaran glacially influenced strata, found outside of North America, although loosely constrained, are generally absent by ~550 Ma (Wang R. et al., 2023b; Wang R. et al., 2023c). Conspicuously, there is an increase in nearshore depositional environment carbonate quantity that is dominantly limestone from 550-545 Ma (Figs 2-3). There is an overall decreasing trend in $\delta^{13}C$ values that begins at ~552 Ma and both slope/basin and outer shelf categories exhibit averages that may be related to potential excursions at the end of the Ediacaran (Yang et al., 2021), though it is far less definitive than that of the SW-CIE (Fig. 4B-C). The increase in nearshore carbonate quantity is also coincident with final pulses of the CIMP/Laurentian rifting (Condie et al., 2021; Ernst et al., 2021) and the first occurrences of the oldest known biomineralizers (and presumed metazoans) such as *Cloudinia*, *Namacalathus*, or *Shaanxilithes* (Xiao and Narbonne, 2020; Shore et al., 2021; Wang et al., 2021). Interestingly, these latest Ediacaran biomineralizers are currently some of the oldest Ediacaran biota taxa to be found within carbonate lithologies, whereas most of the rest of the Ediacaran biota are found as molds within siliciclastic rocks (Xiao and Narbonne, 2020; Droser et al., 2022). We do not assert that expansion of nearshore carbonate environments directly drove the advent of metazoan biomineralization, but rather that the coincident change in depositional environment characteristics may have helped to shape circumstances in which biomineralization and colonization of carbonate-rich shallow marine environments was advantageous. Tectonic and glacioeustatic driven sea level rise may have increased shallow marine habitable environments and/or non-carbonate dominated shallow marine settings may have become less hospitable due to redox changes, thus providing the impetus for biological adaptation and expansion into carbonate depositional environments (Evans et al., 2022; Caxito et al., 2024; Zhang et al., 2024).

More broadly, it is worth noting that biodiversity trends of the informal Ediacaran biota's Avalon, White Sea, and Nama divisions are broadly coincident with the environmental/climactic transitions presented and discussed thus far (Evans et al., 2022; Fig. 6 of Bowyer et al., 2024; Segessenman and Peters, 2024): 1) Avalon peak generic richness reaches maximum diversity coincident with the SW-CIE's recovery, but decreases sharply as carbonate quantity sharply decreases; 2) White Sea generic richness abruptly increases coincident with the second pulse of carbonate quantity and decreases/transitions to the Nama at the ~550 Ma end of the Luoquan glaciation; 3) Nama generic richness is never as high as that of the Avalon or White Sea, but its peak is nominally coincident with the final pulse of carbonate quantity during the latest Ediacaran; 4) The Ediacaran biota declines across the Ediacaran-Cambrian boundary, coincident with decreases in carbonate quantity, regression (Shahkarami et al., 2020), and the advent of Cambrian small shelly faunas (Bowyer et al., 2024). However, the Ediacaran biota has largely been found in non-carbonate lithologies and the Avalon assemblage is generally associated with deeper marine settings (Xiao and Narbonne, 2020), so we are not attributing a direct connection between carbonate depositional environment and Ediacaran biodiversity (at least not for the Avalon or White Sea assemblages). Increases in accommodation may have promoted greater burial of organic carbon within long-term reservoirs of continental margins, thus enabling atmospheric and/or oceanic oxygen buildup (e.g., Husson and Peters, 2017; Zhang et al., 2019;

Cao et al., 2020; Li et al., 2020; Shi et al., 2023), a potential necessity for evolutionary developments of the Ediacaran biota (Sperling et al., 2015; Evans et al., 2018; Evans et al., 2022). Ediacaran organisms themselves may have played a role in shaping environments to better suit them, with fluid dynamics analyses suggesting that early Ediacaran communities may have promoted ocean O_2 ventilation (Schiffbauer and Bykova, 2024) and increasing ecosystem engineering by putative metazoans in the late Ediacaran may have promoted macroevolutionary change across the Ediacaran-Cambrian boundary (Mussini and Dunn, 2024). However, it should be noted that redox proxies, physiology, and life habits of Ediacaran organisms are not straight-forward to interpret and are complex, challenging topics that are areas of ongoing development (e.g., Boag et al., 2018; Cherry et al., 2022; Gong et al., 2023; Mussini and Dunn, 2024). Despite the complexities, Ediacaran carbonate quantity and geochemistry may serve as proxies signifying common cause mechanisms known from the Phanerozoic of glacioeustacy, rifting, and supercontinent amalgamation that drove Ediacaran marine depositional environment changes, global climate shifts, and macroevolution.

While there are still many unknowns regarding the Ediacaran and age constraints, there is at least one more known factor that likely contributed to the evolution of Earth-systems dynamics in the Ediacaran and Cambrian Periods that should be included in considerations of the SW-CIE, global climate dynamics, and Ediacaran macroevolution. An identified ultra-low time-averaged field intensity (UL-TAFI) of Earth's magnetic field, potentially related to a late inner core nucleation and estimated to be 10-30 times weaker than in the modern, appears to reach a minimum in the middle Ediacaran and continues through to the middle Cambrian (Huang et al., 2024). This is a seemingly unique event in Earth history that overlaps with the SW-CIE, the Ediacaran biota's appearance, potential climactic shifts in the middle to late Ediacaran, and the

Cambrian radiation of metazoans (Bono et al., 2019; Li et al., 2023; Huang et al., 2024). The UL-TAFI may have allowed for an increase in the rate of hydrogen stripping from the upper atmosphere by solar wind. This in turn could have led to oxygenation of Earth's atmosphere, perhaps contributing to the expression of the SW-CIE and the appearance of shallow marine taxa from the Ediacaran biota (Urey, 1952; Siscoe and Chen, 1975; Meert et al., 2016; Huang et al., 2024). This has also contributed to the difficulty of developing paleogeographic reconstructions for the Ediacaran, a critical component to assessing the influences of various tectonics on global climate and macroevolution (Domeier et al., 2023). As an emerging area of discussion and research, it remains unclear how the UL-TAFI may have influenced other Earth systems in the Ediacaran. If the UL-TAFI was related to a late-stage inner core nucleation (Bono et al., 2019; Li et al., 2023), how might that have affected mantle convection dynamics that drove tectonic events affecting shallow shelf area, carbonate quantity and geochemistry such as Laurentian rifting, CIMP magmatism, and Gondwana's amalgamation? Could a severely weakened magnetic field have contributed to shifts in global climate dynamics or influenced the development of ozone? How might higher UV exposure in shallow marine environments have shaped the evolution of the Ediacaran biota and early to middle Cambrian faunas? These are all intriguing questions that have been posed (Meert et al., 2016; Pan and Li, 2023) and require further exploration. Although the exact nature of the UL-TAFI's contribution is unknown, it seems unlikely that it did not have any influence and is worth considering for hypotheses concerning Earth systems evolution during the middle Ediacaran to middle Cambrian.

5. Conclusions

Continental scale tectonic mechanisms such as orogenic silicate weathering and LIP magmatism/weathering are mechanisms that have been tied to both cooling and warming of global climate in the Phanerozoic via the release and drawdown of CO_2, including Pangea amalgamation as a driver of the Late Paleozoic Ice Age and Himalayan mountain-building as a driver of Cenozoic glaciation (Condie et al., 2021; Youbi et al., 2021; Nance, 2022). However, other factors unique to each of these periods/events are also considered to be important contributors to how effective tectonics are in levering global climate. Are there other major components to the outgassing, such as elevated sulfate? What is the composition of emplaced LIPs and how quickly do they weather (these first two points are tied to initiation of Sturtian glaciation; e.g., Macdonald and Swanson-Hysell, 2023)? How close to the equator was CO_2 outgassing (also tied to the initiation of Cryogenian glaciation)? What is the composition of rock being weathered during orogenic events (e.g., Tonian evaporite weathering related to SW-CIE; Shields et al., 2019) or of LIP magmas that are emplaced and weathered? The biosphere has also played a major role in periods of major CO_2 drawdown (and pO_2 buildup), such as the burial of organic matter in widespread anoxic swamps in the Permo-Carboniferous (Kent and Muttoni, 2020). Some truly unique drivers have been proposed for the end-Ordovician glaciation in the form of an orbital debris ring caused by a near-Earth asteroid breakup shading the equator (Tomkins et al., 2024). The dynamic interplay of the global climate levers listed above highlights that although familiar drivers affect Earth's climate throughout its history, every period has unique dynamics that change the balance and sensitivity of feedback mechanisms contributing to Earth systems evolution. The Ediacaran appears to have been a unique global state of major continental rifting coeval with major orogenesis that potentially shaped global climate, depositional environments, and macroevolutionary trends of the oldest known metazoans, the signals of which may be reflected in continental scale carbonate deposition quantity and geochemistry.

Changes in the estimated quantities of the preserved carbonate record can be difficult to interpret, as continental scale controls on deposition and preservation are often complex combinations of multiple global and local scale controls in addition to potential post-deposition deformation and erosion of strata that were preserved. However, by analyzing carbonate quantity with regards to the unique geologic context of the Ediacaran and their depositional environments, we found that patterns of North American carbonate deposition are largely consistent with existing hypotheses of Ediacaran tectonic forcings that may have influenced long term sea level, climate, marine redox states, and macroevolution. Additionally, a mid-Ediacaran carbonate quantity maximum that is dominantly dolostone increases across all categories of depositional environments and is coeval with the hallmark negative $\delta^{13}C$ values of the SW-CIE, which supports the idea of a continental-scale transgressive event that was, at least in part, driven by global tectonics and glacioeustacy. These findings indicate that the magnitude of the SW-CIE excursion may have had at least some contribution from global carbon cycling perturbation and that the uniquely extreme magnitude of the SW-CIE may be a mixed signal of oceanic DIC $\delta^{13}C$ and proposed mechanisms that could have decoupled shallow marine carbonate $\delta^{13}C$. The Ediacaran biota’s oldest known occurrences also coincide with the Ediacaran carbonate maximum, and the first occurrences of Ediacaran biomineralizers coincide with the final pulse of dominantly nearshore carbonate quantity, potentially supporting common cause drivers of carbonate quantity and macroevolution during the mid-to-late Ediacaran. Ediacaran carbonate quantity and geochemistry, when combined with results of studies compiling and establishing the timings of potentially globally influential events (e.g., Gondwana amalgamation, CIMP magmatism, and others discussed previously), may serve as a rough proxy for long-term climate and tectonic dynamics that shaped the evolution of Earth's oldest complex macroscopic organisms. While the results presented here are generally consistent with studies that include global compilations of relevant key stratigraphic sections, the extent to which the aggregate quantity and geochemistry of carbonates from the Ediacaran System of North America are representative of the Ediacaran Earth remains unknown. Expansion of this dataset and the analyses presented here to include other continents and geochemical data, continued establishment of new geochronologic constraints, and further geochemical analysis of proxies that enable reconstruction of Ediacaran paleoclimate will further enhance our understanding of Earth systems evolution during the dawn of animal life.

Acknowledgements

DCS was supported in part by the Dean L. Morgridge graduate fellowship, the University of Wisconsin-Madison Dept. of Geoscience, and the George Mason University Atmospheric, Oceanic, and Earth Sciences Dept. We thank J. Husson and B. Hupp for feedback on early drafts of this manuscript. We also thank G. Gilleaudeau and A.J. Kaufman for insightful feedback on topics presented in this manuscript. Macrostrat infrastructure development was supported by US National Science Foundation EAR-1150082 and EarthCube ICER-1440312.

References

Ahm, A.-S.C., Bjerrum, C.J., Hoffman, P.F., Macdonald, F.A., Maloof, A.C., Rose, C.V., Strauss, J.V., Higgins, J.A., 2021. The Ca and Mg isotope record of the Cryogenian

Trezona carbon isotope excursion. Earth and Planetary Science Letters 568, 117002. https://doi.org/10.1016/j.epsl.2021.117002

Ahm, A.-S.C., Husson, J.M., 2022. Local and global controls on carbon isotope chemostratigraphy: Cambridge University Press. https://doi.org/10.1017/9781009028882

Ahm, A.-S.C., Maloof, A.C., Macdonald, F.A., Hoffman, P.F., Bjerrum, C.J., Bold, U., Rose, C.V., Strauss, J.V., Higgins, J.A., 2019. An early diagenetic deglacial origin for basal Ediacaran "cap dolostones." Earth and Planetary Science Letters 506, 292–307. https://doi.org/10.1016/j.epsl.2018.10.046

Alcott, L.J., Walton, C., Planavsky, N.J., Shorttle, O., Mills, B.J.W., 2024. Crustal carbonate build-up as a driver for Earth's oxygenation. Nature Geoscience 17, 458–464. https://doi.org/10.1038/s41561-024-01417-1

Aleinikoff, J.N., Zartman, R.E., Walter, M., Rankin, D.W., Lyttle, P.T., Burton, W.C., 1995. U-Pb Ages of Metarhyolites of the Catoctin and Mount Rogers Formations, Central and Southern Appalachians: Evidence for Two Pulses of Iapetan Rifting. American Journal of Science 295, 428–454. https://doi.org/10.2475/ajs.295.4.428

Beranek, L.P., Hutter, A.D., Pearcey, S., James, C., Langor, V., Pike, C., Goudie, D., Oldham, L., 2023. New evidence for the Baltican cratonic affinity and Tonian to Ediacaran tectonic evolution of West Avalonia in the Avalon Peninsula, Newfoundland, Canada. Precambrian Research 390, 107046. https://doi.org/10.1016/j.precamres.2023.107046

Bergmann, K.D., Zentmyer, R.A., Fischer, W.W., 2011. The stratigraphic expression of a large negative carbon isotope excursion from the Ediacaran Johnnie Formation, Death Valley. Precambrian Research 188, 45–56. https://doi.org/10.1016/j.precamres.2011.03.014

Boag, T.H., Stockey, R.G., Elder, L.E., Hull, P.M., Sperling, E.A., 2018. Oxygen, temperature and the deep-marine stenothermal cradle of Ediacaran evolution. Proceedings of the Royal Society B 285, 20181724. https://doi.org/10.1098/rspb.2018.1724

Bobrovskiy, I., Hope, J.M., Ivantsov, A., Nettersheim, B.J., Hallmann, C., Brocks, J.J., 2018. Ancient steroids establish the Ediacaran fossil *Dickinsonia* as one of the earliest animals. Science 361, 1246–1249. https://doi.org/10.1126/science.aat7228

Bono, R.K., Tarduno, J.A., Nimmo, F., Cottrell, R.D., 2019. Young inner core inferred from Ediacaran ultra-low geomagnetic field intensity. Nature Geoscience 12, 143–147. https://doi.org/10.1038/s41561-018-0288-0

Boulila, S., Peters, S.E., Müller, R.D., Haq, B.U., Hara, N., 2023. Earth's interior dynamics drive marine fossil diversity cycles of tens of millions of years. Proceedings of the National Academy of Sciences of the United States of America 120, e2221149120. https://doi.org/10.1073/pnas.2221149120

Bowyer, F.T., Uahengo, C.-I., Kaputuaza, K., Ndeunyema, J., Yilales, M., Alexander, R.D., Curtis, A., Wood, R.A., 2023. Constraining the onset and environmental setting of metazoan biomineralization: The Ediacaran Nama Group of the Tsaus Mountains, Namibia. Earth and Planetary Science Letters 620, 118336. https://doi.org/10.1016/j.epsl.2023.118336

Bowyer, F.T., Wood, R.A., Yilales, M., 2024. Sea level controls on Ediacaran-Cambrian animal radiations. Sci. Adv. 10, eado6462. https://doi.org/10.1126/sciadv.ado6462

Bowyer, F.T., Zhuravlev, A.Y., Wood, R., Shields, G.A., Zhou, Y., Curtis, A., Poulton, S.W., Condon, D.J., Yang, C., Zhu, M., 2022. Calibrating the temporal and spatial dynamics of the Ediacaran - Cambrian radiation of animals. Earth-Science Reviews 225, 103913. https://doi.org/10.1016/j.earscirev.2021.103913

Brendan Murphy, J., Damian Nance, R., Johnston, S.T., Casas, J.M., Cawood, P.A., Matheson, E.J., Pufahl, P.K., Dan, W., Javier Álvaro, J., Heron, P.J., Strachan, R.A., 2024. Speculations on the Paleozoic legacy of Gondwana amalgamation. Gondwana Research 129, 107–131. https://doi.org/10.1016/j.gr.2023.12.002

Busch, J.F., Boag, T.H., Sperling, E.A., Rooney, A.D., Feng, X., Moynihan, D.P., Strauss, J.V., 2023. Integrated Litho-, Chemo- and Sequence Stratigraphy of the Ediacaran Gametrail Formation Across a Shelf-Slope Transect in the Wernecke Mountains, Yukon, Canada. American Journal of Science 323. https://doi.org/10.2475/001c.74874

Busch, J.F., Hodgin, E.B., Ahm, A.-S.C., Husson, J.M., Macdonald, F.A., Bergmann, K.D., Higgins, J.A., Strauss, J.V., 2022. Global and local drivers of the Ediacaran Shuram carbon isotope excursion. Earth and Planetary Science Letters 579, 117368. https://doi.org/10.1016/j.epsl.2022.117368

Busch, J.F., Rooney, A.D., Meyer, E.E., Town, C.F., Moynihan, D.P., Strauss, J.V., 2021. Late Neoproterozoic – early Paleozoic basin evolution in the Coal Creek inlier of Yukon, Canada: implications for the tectonic evolution of northwestern Laurentia. Canadian Journal of Earth Sciences 58, 355–377. https://doi.org/10.1139/cjes-2020-0132

Canfield, D.E., Knoll, A.H., Poulton, S.W., Narbonne, G.M., Dunning, G.R., 2020. Carbon isotopes in clastic rocks and the Neoproterozoic carbon cycle. American Journal of Science 320, 97–124. https://doi.org/10.2475/02.2020.01

Cantine, M.D., Knoll, A.H., Bergmann, K.D., 2020. Carbonates before skeletons: A database approach. Earth-Science Reviews 201, 103065. https://doi.org/10.1016/j.earscirev.2019.103065

Cantine, M.D., Rooney, A.D., Knoll, A.H., Gómez-Pérez, I., Al Baloushi, B., Bergmann, K.D., 2024. Chronology of Ediacaran sedimentary and biogeochemical shifts along eastern Gondwanan margins. Communications Earth & Environment 5, 520. https://doi.org/10.1038/s43247-024-01630-1

Cao, M., Daines, S.J., Lenton, T.M., Cui, H., Algeo, T.J., Dahl, T.W., Shi, W., Chen, Z.-Q., Anbar, A., Zhou, Y.-Q., 2020. Comparison of Ediacaran platform and slope δ238U records in South China: Implications for global-ocean oxygenation and the origin of the Shuram Excursion. Geochimica et Cosmochimica Acta 287, 111–124. https://doi.org/10.1016/j.gca.2020.04.035

Caxito, F., Lana, C., Frei, R., Uhlein, G.J., Sial, A.N., Dantas, E.L., Pinto, A.G., Campos, F.C., Galvão, P., Warren, L.V., Okubo, J., Ganade, C.E., 2021. Goldilocks at the dawn of complex life: mountains might have damaged Ediacaran–Cambrian ecosystems and prompted an early Cambrian greenhouse world. Scientific Reports 11, 20010. https://doi.org/10.1038/s41598-021-99526-z

Caxito, F.A., Sperling, E., Fazio, G., Adorno, R.R., Denezine, M., Carmo, D.A.D., Giorgioni, M., Uhlein, G.J., Sial, A.N., 2024. A shift in redox conditions near the Ediacaran/Cambrian transition and its possible influence on early animal evolution, Corumbá Group, Brazil. Geoscience Frontiers 15, 101810. https://doi.org/10.1016/j.gsf.2024.101810

Cherry, L.B., Gilleaudeau, G.J., Grazhdankin, D.V., Romaniello, S.J., Martin, A.J., Kaufman, A.J., 2022. A diverse Ediacara assemblage survived under low-oxygen conditions. Nature Communications 13, 7306. https://doi.org/10.1038/s41467-022-35012-y

Cochrane, D.J.W., Navarro, L., Arnott, R.W.C., 2019. Sedimentological and geochemical evolution of an Ediacaran mixed carbonate-siliciclastic continental slope system, Windermere Supergroup, southern Canadian Cordillera, British Columbia, Canada. Precambrian Research 327, 47–67. https://doi.org/10.1016/j.precamres.2019.02.021

Condie, K.C., Pisarevsky, S.A., Puetz, S.J., 2021. LIPs, orogens and supercontinents: The ongoing saga. Gondwana Research 96, 105–121. https://doi.org/10.1016/j.gr.2021.05.002

Conley, D.J., Carey, J.C., 2015. Silica cycling over geologic time. Nature Geoscience 8, 431–432. https://doi.org/10.1038/ngeo2454

Conley, D.J., Frings, P.J., Fontorbe, G., Clymans, W., Stadmark, J., Hendry, K.R., Marron, A.O., De La Rocha, C.L., 2017. Biosilicification Drives a Decline of Dissolved Si in the Oceans through Geologic Time. Frontiers in Marine Science 4, 397. https://doi.org/10.3389/fmars.2017.00397

Corsetti, F.A., Hagadorn, J.W., 2000. Precambrian-Cambrian transition: Death Valley, United States. Geology 28, 299–302. https://doi.org/10.1130/0091-7613(2000)28<299:PTDVUS>2.0.CO;2

Corsetti, F.A., J. Kaufman, A.J., 2003. Stratigraphic investigations of carbon isotope anomalies and Neoproterozoic ice ages in Death Valley, California. Geological Society of America Bulletin 115, 916–932. https://doi.org/10.1130/B25066.1

Corsetti, F.A., Kaufman, A.J., 1994. Chemostratigraphy of Neoproterozoic-Cambrian Units, White-Inyo Region, Eastern California and Western Nevada: Implications for Global

Correlation and Faunal Distribution. PALAIOS 9, 211–219. https://doi.org/10.2307/3515107

Cramer, B.D., Jarvis, I., 2020. Carbon Isotope Stratigraphy, in: Gradstein, F.M., Ogg, J.G., Schmitz, M.D., Ogg, G.M. (Eds.), Geologic Time Scale 2020. Elsevier, pp. 309–343. https://doi.org/10.1016/B978-0-12-824360-2.00011-5

Creveling, J.R., Bergmann, K.D., Grotzinger, J.P., 2016. Cap carbonate platform facies model, Noonday Formation, SE California. Geological Society of America Bulletin 128, 1249–1269. https://doi.org/10.1130/B31442.1

Creveling, J.R., Mitrovica, J.X., 2014. The sea-level fingerprint of a Snowball Earth deglaciation. Earth and Planetary Science Letters 399, 74–85. https://doi.org/10.1016/j.epsl.2014.04.029

Cui, H., Kaufman, A.J., Xiao, S., Zhou, C., Liu, X.-M., 2017. Was the Ediacaran Shuram Excursion a globally synchronized early diagenetic event? Insights from methane-derived authigenic carbonates in the uppermost Doushantuo Formation, South China. Chemical Geology 450, 59–80. https://doi.org/10.1016/j.chemgeo.2016.12.010

Cui, H., Kaufman, A.J., Xiao, S., Zhou, C., Zhu, M., Cao, M., Loyd, S., Crockford, P., Liu, X.-M., Goderis, S., Wang, W., Guan, C., 2022. Dynamic interplay of biogeochemical C, S and Ba cycles in response to the Shuram oxygenation event. Journal of the Geological Society of London 179, jgs2021-081. https://doi.org/10.1144/jgs2021-081

Cui, H., Kitajima, K., Orland, I.J., Xiao, S., Baele, J.-M., Kaufman, A.J., Denny, A., Zhou, C., Spicuzza, M.J., Fournelle, J.H., Valley, J.W., 2021. Deposition or diagenesis? Probing the Ediacaran Shuram excursion in South China by SIMS. Global and Planetary Change 206, 103591. https://doi.org/10.1016/j.gloplacha.2021.103591

Darroch, S.A.F., Cribb, A.T., Buatois, L.A., Germs, G.J.B., Kenchington, C.G., Smith, E.F., Mocke, H., O'Neil, G.R., Schiffbauer, J.D., Maloney, K.M., Racicot, R.A., Turk, K.A., Gibson, B.M., Almond, J., Koester, B., Boag, T.H., Tweedt, S.M., Laflamme, M., 2021. The trace fossil record of the Nama Group, Namibia: Exploring the terminal Ediacaran roots of the Cambrian explosion. Earth-Science Reviews 212, 103435. https://doi.org/10.1016/j.earscirev.2020.103435

Derry, L.A., 2010. A burial diagenesis origin for the Ediacaran Shuram–Wonoka carbon isotope anomaly. Earth and Planetary Science Letters 294, 152–162. https://doi.org/10.1016/j.epsl.2010.03.022

Dewey, J., Spall, H., 1975. Pre-Mesozoic plate tectonics: How far back in Earth history can the Wilson Cycle be extended? Geology 3, 422–424. https://doi.org/10.1130/0091-7613(1975)3<422:PPTHFB>2.0.CO;2

Dodd, M.S., Shi, W., Li, C., Zhang, Z., Cheng, M., Gu, H., Hardisty, D.S., Loyd, S.J., Wallace, M.W., vS. Hood, A., Lamothe, K., Mills, B.J.W., Poulton, S.W., Lyons, T.W., 2023. Uncovering the Ediacaran phosphorus cycle. Nature 618, 974–980. https://doi.org/10.1038/s41586-023-06077-6

Domeier, M., Robert, B., Meert, J.G., Kulakov, E.V., McCausland, P.J.A., Trindade, R.I.F., Torsvik, T.H., 2023. The enduring Ediacaran paleomagnetic enigma. Earth-Science Reviews 242, 104444. https://doi.org/10.1016/j.earscirev.2023.104444

Droser, M.L., Evans, S.D., Tarhan, L.G., Surprenant, R.L., Hughes, I.V., Hughes, E.B., Gehling, J.G., 2022. What Happens Between Depositional Events, Stays Between Depositional Events: The Significance of Organic Mat Surfaces in the Capture of Ediacara

Communities and the Sedimentary Rocks That Preserve Them. Frontiers in Earth Science 10, 826353. https://doi.org/10.3389/feart.2022.826353

Ernst, R.E., Bond, D.P.G., Zhang, S., Buchan, K.L., Grasby, S.E., Youbi, N., El Bilali, H., Bekker, A., Doucet, L.S., 2021. Large Igneous Province Record Through Time and Implications for Secular Environmental Changes and Geological Time-Scale Boundaries, in: Ernst, R.E., Dickson, A.J., Bekker, A. (Eds.), Geophysical Monograph Series. Wiley, pp. 1–26. https://doi.org/10.1002/9781119507444.ch1

Evans, S.D., Diamond, C.W., Droser, M.L., Lyons, T.W., 2018. Dynamic oxygen and coupled biological and ecological innovation during the second wave of the Ediacara Biota. Emerging Topics in Life Sciences 2, 223–233. https://doi.org/10.1042/ETLS20170148

Evans, S.D., Tu, C., Rizzo, A., Surprenant, R.L., Boan, P.C., McCandless, H., Marshall, N., Xiao, S., Droser, M.L., 2022. Environmental drivers of the first major animal extinction across the Ediacaran White Sea-Nama transition. Proceedings of the National Academy of Sciences of the United States of America 119, e2207475119. https://doi.org/10.1073/pnas.2207475119

Eyster, A., Ferri, F., Schmitz, M.D., Macdonald, F.A., 2018. One diamictite and two rifts: Stratigraphy and geochronology of the Gataga Mountain of northern British Columbia. American Journal of Science 318, 167–207. https://doi.org/10.2475/02.2018.1

Faehnrich, K., McClelland, W.C., Webb, L., Kośmińska, K., Strauss, J.V., 2023. Late Ediacaran–early Cambrian rifting along the northern margin of Laurentia: constraints from the Yelverton Formation of Ellesmere Island, Canada. Canadian Journal of Earth Sciences 60, 1597–1626. https://doi.org/10.1139/cjes-2023-0020

Fairchild, I., Hambrey, M., 1995. Vendian basin evolution in East Greenland and NE Svalbard. Precambrian Research 73, 217–233. https://doi.org/10.1016/0301-9268(94)00079-7

Fan, H., Chen, Z., Zhang, F., Zhu, C., Du, S., Zhang, Y., Wen, H., Khan, D., Algeo, T.J., 2025. Seawater temperatures during the early to middle Ediacaran: Phosphate oxygen isotope records. Chemical Geology 678, 122642. https://doi.org/10.1016/j.chemgeo.2025.122642

Fang, Y., Hobbs, F., Yang, Y., Xu, H., 2023. Dissolved silica-driven dolomite precipitation in the Great Salt Lake, Utah, and its implication for dolomite formation environments. Sedimentology 70, 1328–1347. https://doi.org/10.1111/sed.13081

Fang, Y., Xu, H., 2022a. Dissolved silica-catalyzed disordered dolomite precipitation. American Mineralogist 107, 443–452. https://doi.org/10.2138/am-2021-7474

Fang, Y., Xu, H., 2022b. Coupled dolomite and silica precipitation from continental weathering during deglaciation of the Marinoan Snowball Earth. Precambrian Research 380, 106824. https://doi.org/10.1016/j.precamres.2022.106824

Fitzgerald, D.M., Narbonne, G.M., Pufahl, P.K., Dalrymple, R.W., 2024. The Mall Bay Formation (Ediacaran) and the protracted onset of the Gaskiers glaciation in Newfoundland, Canada. Precambrian Research 405, 107369. https://doi.org/10.1016/j.precamres.2024.107369

Ganade De Araujo, C.E., Rubatto, D., Hermann, J., Cordani, U.G., Caby, R., Basei, M.A.S., 2014. Ediacaran 2,500-km-long synchronous deep continental subduction in the West Gondwana Orogen. Nature Communications 5, 5198. https://doi.org/10.1038/ncomms6198

Gong, Z., Li, M., 2020. Astrochronology of the Ediacaran Shuram carbon isotope excursion, Oman. Earth and Planetary Science Letters 547, 116462. https://doi.org/10.1016/j.epsl.2020.116462

Gong, Z., Wei, G., Fakhraee, M., Alcott, L.J., Jiang, L., Zhao, M., Planavsky, N.J., 2023. Revisiting marine redox conditions during the Ediacaran Shuram carbon isotope excursion. Geobiology 21, 407–420. https://doi.org/10.1111/gbi.12547

Gostin, V.A., McKirdy, D.M., Webster, L.J., Williams, G.E., 2010. Ediacaran ice-rafting and coeval asteroid impact, South Australia: insights into the terminal Proterozoic environment. Australian Journal of Earth Sciences 57, 859–869. https://doi.org/10.1080/08120099.2010.509408

Green, T., Renne, P.R., Keller, C.B., 2022. Continental flood basalts drive Phanerozoic extinctions. Proceedings of the National Academy of Sciences of the United States of America 119, e2120441119. https://doi.org/10.1073/pnas.2120441119

Grossman, E.L., Joachimski, M.M., 2020. Oxygen Isotope Stratigraphy, in: Gradstein, F.M., Ogg, J.G., Schmitz, M.D., Ogg, G.M. (Eds.), Geologic Time Scale 2020. Elsevier, pp. 279–307. https://doi.org/10.1016/B978-0-12-824360-2.00010-3

Grotzinger, J.P., Fike, D.A., Fischer, W.W., 2011. Enigmatic origin of the largest-known carbon isotope excursion in Earth's history. Nature Geoscience 4, 285–292. https://doi.org/10.1038/ngeo1138

Gu, H., Hu, J., Cheng, M., Wang, H., Dodd, M.S., Zhang, Z., Algeo, T.J., Li, C., 2024. Heterogeneous coupling of δ13Corg and δ13Ccarb during the Shuram Excursion: Implications for a large dissolved organic carbon reservoir in the Ediacaran ocean. Global and Planetary Change 239, 104466. https://doi.org/10.1016/j.gloplacha.2024.104466

Hagadorn, J.W., Waggoner, B., 2000. Ediacaran Fossils from the southwestern Great Basin, United States. Journal of Paleontology 74, 349-359. https://doi.org/10.1666/0022-3360(2000)074<0349:EFFTSG>2.0.CO;2

Hagen, C.J., Creveling, J.R., 2024. An algorithm-guided Ediacaran global composite δ13Ccarb–Bayesian age model. Palaeogeography, Palaeoclimatology, Palaeoecology 650, 112321. https://doi.org/10.1016/j.palaeo.2024.112321

Halevy, I., Bachan, A., 2017. The geologic history of seawater pH. Science 355, 1069–1071. https://doi.org/10.1126/science.aal4151

Halverson, G., Porter, S., Shields, G., 2020. The Tonian and Cryogenian Periods, in: Gradstein, F.M., Ogg, J.G., Schmitz, M.D., Ogg, G.M. (Eds.), Geologic Time Scale 2020. Elsevier, pp. 495–519. https://doi.org/10.1016/B978-0-12-824360-2.00017-6

Halverson, G.P., Hoffman, P.F., Schrag, D.P., Maloof, A.C., Rice, A.H.N., 2005. Toward a Neoproterozoic composite carbon-isotope record. Geological Society of America Bulletin 117, 1181. https://doi.org/10.1130/B25630.1

Halverson, G.P., Maloof, A.C., Hoffman, P.F., 2004. The Marinoan glaciation (Neoproterozoic) in northeast Svalbard. Basin Research 16, 297–324. https://doi.org/10.1111/j.1365-2117.2004.00234.x

Hannisdal, B., Peters, S.E., 2011. Phanerozoic Earth System Evolution and Marine Biodiversity. Science 334, 1121–1124. https://doi.org/10.1126/science.1210695

Hatcher, R.D., 2010. The Appalachian orogen: A brief summary, in: Tollo, R.P., Bartholomew, M.J., Hibbard, J.P., Karabinos, P.M. (Eds.), From Rodinia to Pangea: The Lithotectonic Record of the Appalachian Region. Geological Society of America Memoirs 206, 1–19. https://doi.org/10.1130/2010.1206(01)

Hebert, C.L., Kaufman, A.J., Penniston-Dorland, S.C., Martin, A.J., 2010. Radiometric and stratigraphic constraints on terminal Ediacaran (post-Gaskiers) glaciation and metazoan evolution. Precambrian Research 182, 402–412. https://doi.org/10.1016/j.precamres.2010.07.008

Hodgin, E.B., Nelson, L.L., Wall, C.J., Barrón-Díaz, A.J., Webb, L.C., Schmitz, M.D., Fike, D.A., Hagadorn, J.W., Smith, E.F., 2021. A link between rift-related volcanism and end-Ediacaran extinction? Integrated chemostratigraphy, biostratigraphy, and U-Pb geochronology from Sonora, Mexico. Geology 49, 115–119. https://doi.org/10.1130/G47972.1

Hoffman, P.F., 2011. Strange bedfellows: glacial diamictite and cap carbonate from the Marinoan (635 Ma) glaciation in Namibia. Sedimentology 58, 57–119. https://doi.org/10.1111/j.1365-3091.2010.01206.x

Hoffman, P.F., Halverson, G.P., Domack, E.W., Maloof, A.C., Swanson-Hysell, N.L., Cox, G.M., 2012. Cryogenian glaciations on the southern tropical paleomargin of Laurentia (NE Svalbard and East Greenland), and a primary origin for the upper Russøya (Islay) carbon isotope excursion. Precambrian Research 206–207, 137–158. https://doi.org/10.1016/j.precamres.2012.02.018

Hoffman, P.F., Kaufman, A.J., Halverson, G.P., Schrag, D.P., 1998. A Neoproterozoic Snowball Earth. Science 281, 1342–1346. https://doi.org/10.1126/science.281.5381.1342

Hoffman, P.F., Li, Z.-X., 2009. A palaeogeographic context for Neoproterozoic glaciation. Palaeogeography, Palaeoclimatology, Palaeoecology 277, 158–172. https://doi.org/10.1016/j.palaeo.2009.03.013

Hoffman, P.F., Schrag, D.P., 2002. The snowball Earth hypothesis: testing the limits of global change. Terra Nova 14, 129–155. https://doi.org/10.1046/j.1365-3121.2002.00408.x

Hohmann, N., Koelewijn, J.R., Burgess, P., Jarochowska, E., 2024. Identification of the mode of evolution in incomplete carbonate successions. BMC Ecology and Evolution 24, 113. https://doi.org/10.1186/s12862-024-02287-2

Huang, W., Tarduno, J.A., Zhou, T., Ibañez-Mejia, M., Dal Olmo-Barbosa, L., Koester, E., Blackman, E.G., Smirnov, A.V., Ahrendt, G., Cottrell, R.D., Kodama, K.P., Bono, R.K., Sibeck, D.G., Li, Y.-X., Nimmo, F., Xiao, S., Watkeys, M.K., 2024. Near-collapse of the geomagnetic field may have contributed to atmospheric oxygenation and animal radiation in the Ediacaran Period. Nature Communications Earth & Environment 5, 207. https://doi.org/10.1038/s43247-024-01360-4

Husson, J.M., Coogan, L.A., 2023. River chemistry reveals a large decrease in dolomite abundance across the Phanerozoic. Geochemical Perspectives Letters 26, 1–6. https://doi.org/10.7185/geochemlet.2316

Husson, J.M., Linzmeier, B.J., Kitajima, K., Ishida, A., Maloof, A.C., Schoene, B., Peters, S.E., Valley, J.W., 2020. Large isotopic variability at the micron-scale in ‘Shuram’ excursion carbonates from South Australia. Earth and Planetary Science Letters 538, 116211. https://doi.org/10.1016/j.epsl.2020.116211

Husson, J.M., Peters, S.E., 2017. Atmospheric oxygenation driven by unsteady growth of the continental sedimentary reservoir. Earth and Planetary Science Letters 460, 68–75. https://doi.org/10.1016/j.epsl.2016.12.012

Ineson, J.R., Peel, J.S., Willman, S., Rugen, E.J., Sønderholm, M., Frykman, P., 2024. Lithostratigraphy of the Portfjeld Group (Ediacaran – lowermost Cambrian) of North Greenland. GEUS Bulletin 57. https://doi.org/10.34194/geusb.v57.8375

Isson, T.T., Planavsky, N.J., 2018. Reverse weathering as a long-term stabilizer of marine pH and planetary climate. Nature 560, 471–475. https://doi.org/10.1038/s41586-018-0408-4

Isson, T.T., Planavsky, N.J., Coogan, L.A., Stewart, E.M., Ague, J.J., Bolton, E.W., Zhang, S., McKenzie, N.R., Kump, L.R., 2020. Evolution of the Global Carbon Cycle and Climate Regulation on Earth. Global Biogeochemical Cycles 34, e2018GB006061. https://doi.org/10.1029/2018GB006061

Judd, E.J., Tierney, J.E., Lunt, D.J., Montañez, I.P., Huber, B.T., Wing, S.L., Valdes, P.J., 2024. A 485-million-year history of Earth's surface temperature. Science 385, eadk3705. https://doi.org/10.1126/science.adk3705

Kendall, B.S., Creaser, R.A., Ross, G.M., Selby, D., 2004. Constraints on the timing of Marinoan "Snowball Earth" glaciation by 187Re–187Os dating of a Neoproterozoic, post-glacial black shale in Western Canada. Earth and Planetary Science Letters 222, 729–740. https://doi.org/10.1016/j.epsl.2004.04.004

Kent, D.V., Muttoni, G., 2020. Pangea B and the Late Paleozoic Ice Age. Palaeogeography, Palaeoclimatology, Palaeoecology 553, 109753. https://doi.org/10.1016/j.palaeo.2020.109753

Keppie, J.D., Dostal, J., Murphy, J.B., 1979. Petrology of the Late Precambrian Fourchu Group in the Louisbourg Area, Cape Breton Island: Nova Scotia Department of Mines and Energy 79-1, 18 p.

Keppie, J.D., Keppie, D.F., 2024. Review and tectonic interpretation of Precambrian Avalonia. Geological Society of London Special Publications 542, 149–165. https://doi.org/10.1144/SP542-2022-356

Kim, J., Kimura, Y., Puchala, B., Yamazaki, T., Becker, U., Sun, W., 2023. Dissolution enables dolomite crystal growth near ambient conditions. Science 382, 915–920. https://doi.org/10.1126/science.adi3690

Kirschvink, J.L., 2023. A movable beast: glaciation in the Ediacaran. National Science Review 10, nwad153. https://doi.org/10.1093/nsr/nwad153

Knoll, A.H., Walter, M.R., Narbonne, G.M., Christie-Blick, N., 2006. The Ediacaran Period: a new addition to the geologic time scale. Lethaia 39, 13–30. https://doi.org/10.1080/00241160500409223

Kump, L.R., Arthur, M.A., 1999. Interpreting carbon-isotope excursions: carbonates and organic matter. Chemical Geology 161, 181–198. https://doi.org/10.1016/S0009-2541(99)00086-8

Laakso, T.A., Schrag, D.P., 2020. The role of authigenic carbonate in Neoproterozoic carbon isotope excursions. Earth and Planetary Science Letters 549, 116534. https://doi.org/10.1016/j.epsl.2020.116534

Land, L.S., 1980. The Isotopic and Trace Element Geochemistry of Dolomite: The State of the Art, in: Zenger, D.H., Dunham, J.B., Ethington, R.L. (Eds.), Concepts and Models of Dolomitization. SEPM (Society for Sedimentary Geology). https://doi.org/10.2110/pec.80.28

Land, L.S., 1998. Failure to Precipitate Dolomite at 25 °C from Dilute Solution Despite 1000-Fold Oversaturation after 32 Years. Aquatic Geochemistry 4, 361-368. https://doi.org/10.1023/A:1009688315854

Lee, C., Love, G.D., Fischer, W.W., Grotzinger, J.P., Halverson, G.P., 2015. Marine organic matter cycling during the Ediacaran Shuram excursion. Geology G37236.1. https://doi.org/10.1130/G37236.1

Li, M., Wignall, P.B., Dai, X., Hu, M., Song, H., 2021. Phanerozoic variation in dolomite abundance linked to oceanic anoxia. Geology 49, 698–702. https://doi.org/10.1130/G48502.1

Li, R., Zhou, X., Eddy, M.P., Ickert, R.B., Wang, Z., Tang, D., Huang, K.-J., Peng, P., 2024. Stratigraphic evidence for a major unconformity within the Ediacaran System. Earth and Planetary Science Letters 636, 118715. https://doi.org/10.1016/j.epsl.2024.118715

Li, Y.-X., Tarduno, J.A., Jiao, W., Liu, X., Peng, S., Xu, S., Yang, A., Yang, Z., 2023. Late Cambrian geomagnetic instability after the onset of inner core nucleation. Nature Communications 14, 4596. https://doi.org/10.1038/s41467-023-40309-7

Li, Z., Cao, M., Loyd, S.J., Algeo, T.J., Zhao, H., Wang, X., Zhao, L., Chen, Z.-Q., 2020. Transient and stepwise ocean oxygenation during the late Ediacaran Shuram Excursion: Insights from carbonate δ238U of northwestern Mexico. Precambrian Research 344, 105741. https://doi.org/10.1016/j.precamres.2020.105741

Loyd, S.J., Marenco, P.J., Hagadorn, J.W., Lyons, T.W., Kaufman, A.J., Sour-Tovar, F., Corsetti, F.A., 2012. Sustained low marine sulfate concentrations from the Neoproterozoic to the Cambrian: Insights from carbonates of northwestern Mexico and eastern California. Earth and Planetary Science Letters 339–340, 79–94. https://doi.org/10.1016/j.epsl.2012.05.032

Ma, B., Tian, W., Wu, G., Nance, R.D., Zhao, Y., Chen, Y., Huang, S., 2022. The subduction-related Great Unconformity in the Tarim intracraton, NW China. Global and Planetary Change 215, 103883. https://doi.org/10.1016/j.gloplacha.2022.103883

Ma, C., Hames, W.E., Foster, D.A., Xiao, W., Mueller, P.A., Steltenpohl, M.G., 2023. Transformation of eastern North America from compression to extension in the Permian–Triassic, in: Whitmeyer, S.J., Williams, M.L., Kellett, D.A., Tikoff, B. (Eds.), Laurentia: Turning Points in the Evolution of a Continent. Geological Society of America, pp. 577–592. https://doi.org/10.1130/2022.1220(28)

Macdonald, F.A., McClelland, W.C., Schrag, D.P., Macdonald, W.P., 2009. Neoproterozoic glaciation on a carbonate platform margin in Arctic Alaska and the origin of the North Slope subterrane. Geological Society of America Bulletin 121, 448–473. https://doi.org/10.1130/B26401.1

Macdonald, F.A., Strauss, J.V., Sperling, E.A., Halverson, G.P., Narbonne, G.M., Johnston, D.T., Kunzmann, M., Schrag, D.P., Higgins, J.A., 2013. The stratigraphic relationship between the Shuram carbon isotope excursion, the oxygenation of Neoproterozoic oceans, and the first appearance of the Ediacara biota and bilaterian trace fossils in northwestern Canada. Chemical Geology 362, 250–272. https://doi.org/10.1016/j.chemgeo.2013.05.032

Macdonald, F.A., Swanson-Hysell, N.L., 2023. The Franklin Large Igneous Province and Snowball Earth Initiation. Elements 19, 296–301. https://doi.org/10.2138/gselements.19.5.296

Macdonald, F.A., Yonkee, W.A., Flowers, R.M., Swanson-Hysell, N.L., 2023. Neoproterozoic of Laurentia, in: Laurentia: Whitmeyer, S.J., Williams, M.L., Kellett, D.A., Tikoff, B. (Eds.), Turning Points in the Evolution of a Continent. Geological Society of America, pp. 331–380. https://doi.org/10.1130/2022.1220(19)

MacLennan, S.A., Eddy, M.P., Merschat, A.J., Mehra, A.K., Crockford, P.W., Maloof, A.C., Southworth, C.S., Schoene, B., 2020. Geologic evidence for an icehouse Earth before the Sturtian global glaciation. Science Advances 6, eaay6647. https://doi.org/10.1126/sciadv.aay6647

McDannell, K.T., Keller, C.B., Guenthner, W.R., Zeitler, P.K., Shuster, D.L., 2022. Thermochronologic constraints on the origin of the Great Unconformity. Proceedings of the National Academy of Sciences of the United States of America 119, e2118682119. https://doi.org/10.1073/pnas.2118682119

McGee, B., Collins, A.S., Trindade, R.I.F., 2013. A Glacially Incised Canyon in Brazil: Further Evidence for Mid-Ediacaran Glaciation? The Journal of Geology 121, 275–287. https://doi.org/10.1086/669979

Meert, J.G., Levashova, N.M., Bazhenov, M.L., Landing, E., 2016. Rapid changes of magnetic Field polarity in the late Ediacaran: Linking the Cambrian evolutionary radiation and increased UV-B radiation. Gondwana Research 34, 149–157. https://doi.org/10.1016/j.gr.2016.01.001

Meert, J.G., Lieberman, B.S., 2008. The Neoproterozoic assembly of Gondwana and its relationship to the Ediacaran–Cambrian radiation. Gondwana Research 14, 5–21. https://doi.org/10.1016/j.gr.2007.06.007

Meyers, S.R., Peters, S.E., 2011. A 56million year rhythm in North American sedimentation during the Phanerozoic. Earth and Planetary Science Letters 303, 174–180. https://doi.org/10.1016/j.epsl.2010.12.044

Miall, A.D., 2016. The valuation of unconformities. Earth-Science Reviews 163, 22–71. https://doi.org/10.1016/j.earscirev.2016.09.011

Middelburg, J.J., Soetaert, K., Hagens, M., 2020. Ocean Alkalinity, Buffering and Biogeochemical Processes. Reviews of Geophysics 58, e2019RG000681. https://doi.org/10.1029/2019RG000681

Moynihan, D.P., Strauss, J.V., Nelson, L.L., Padget, C.D., 2019. Upper Windermere Supergroup and the transition from rifting to continent-margin sedimentation, Nadaleen River area, northern Canadian Cordillera. Geological Society of America Bulletin 131, 1673–1701. https://doi.org/10.1130/B32039.1

Müller, R.D., Dutkiewicz, A., Zahirovic, S., Merdith, A.S., Scotese, C.R., Mills, B.J.W., Ilano, L., Mather, B., 2024. Solid Earth Carbon Degassing and Sequestration Since 1 Billion Years Ago. Geochemistry, Geophysics, Geosystems 25, e2024GC011713. https://doi.org/10.1029/2024GC011713

Murphy, J.B., Nance, R.D., Wu, L., 2023. The provenance of Avalonia and its tectonic implications: a critical reappraisal. Geological Society of London Speical Publications 531, 207–247. https://doi.org/10.1144/SP531-2022-176

Mussini, G., Dunn, F.S., 2024. Decline and fall of the Ediacarans: late-Neoproterozoic extinctions and the rise of the modern biosphere. Biological Reviews 99, 110–130. https://doi.org/10.1111/brv.13014

Myrow, P.M., Kaufman, A.J., 1999. A newly discovered cap carbonate above Varanger-Age glacial deposits in Newfoundland, Canada. Journal of Sedimentary Research 69, 784–793. https://doi.org/10.2110/jsr.69.784

Myrow, P.M., Lamb, M.P., Ewing, R.C., 2018. Rapid sea level rise in the aftermath of a Neoproterozoic snowball Earth. Science 360, 649–651. https://doi.org/10.1126/science.aap8612

Nance, R.D., 2022. The supercontinent cycle and Earth's long-term climate. Annals of the New York Academy of Sciences 1515, 33–49. https://doi.org/10.1111/nyas.14849

Oriolo, S., Oyhantçabal, P., Wemmer, K., Siegesmund, S., 2017. Contemporaneous assembly of Western Gondwana and final Rodinia break-up: Implications for the supercontinent cycle. Geoscience Frontiers 8, 1431–1445. https://doi.org/10.1016/j.gsf.2017.01.009

Pan, Y., Li, J., 2023. On the biospheric effects of geomagnetic reversals. National Science Review 10, nwad070. https://doi.org/10.1093/nsr/nwad070

Peng, S.C., Babcock, L.E., Ahlberg, P., 2020. The Cambrian Period, in: Gradstein, F.M., Ogg, J.G., Schmitz, M.D., Ogg, G.M. (Eds.), Geologic Time Scale 2020. Elsevier, pp. 565–629. https://doi.org/10.1016/B978-0-12-824360-2.00019-X

Peters, S.E., 2008. Environmental determinants of extinction selectivity in the fossil record. Nature 454, 626–629. https://doi.org/10.1038/nature07032

Peters, S.E., 2006. Macrostratigraphy of North America. The Journal of Geology 114, 391–412. https://doi.org/10.1086/504176

Peters, S.E., Husson, J.M., 2018. We need a global comprehensive stratigraphic database: here's a start. The Sedimentary Record 16, 4–9. https://doi.org/10.2110/sedred.2018.1.4

Peters, S.E., Husson, J.M., Czaplewski, J., 2018. Macrostrat: A Platform for Geological Data Integration and Deep-Time Earth Crust Research. Geochemistry, Geophysics, Geosystems 19, 1393–1409. https://doi.org/10.1029/2018GC007467

Peters, S.E., Quinn, D.P., Husson, J.M., Gaines, R.R., 2022. Macrostratigraphy: Insights into Cyclic and Secular Evolution of the Earth-Life System. Annual Review of Earth and Planetary Sciences 50, 419–449. https://doi.org/10.1146/annurev-earth-032320-081427

Peters, S.E., Walton, C.R., Husson, J.M., Quinn, D.P., Shorttle, O., Keller, C.B., Gaines, R.R., 2021. Igneous rock area and age in continental crust. Geology 49, 1235–1239. https://doi.org/10.1130/G49037.1

Petterson, R., Prave, A.R., Wernicke, B.P., Fallick, A.E., 2011. The Neoproterozoic Noonday Formation, Death Valley region, California. Geological Society of America Bulletin 123, 1317–1336. https://doi.org/10.1130/B30281.1

Pu, J.P., Bowring, S.A., Ramezani, J., Myrow, P., Raub, T.D., Landing, E., Mills, A., Hodgin, E., Macdonald, F.A., 2016. Dodging snowballs: Geochronology of the Gaskiers glaciation and the first appearance of the Ediacaran biota. Geology 44, 955–958. https://doi.org/10.1130/G38284.1

Quinn, D.P., Idzikowski, C.R., Peters, S.E., 2024. Building a multi-scale, collaborative, and time-integrated digital crust: The next stage of the Macrostrat data system. Geoscience Data Journal 11, 11–26. https://doi.org/10.1002/gdj3.189

Robert, B., Domeier, M., Jakob, J., 2021. On the origins of the Iapetus Ocean. Earth-Science Reviews 221, 103791. https://doi.org/10.1016/j.earscirev.2021.103791

Rooney, A.D., Cantine, M.D., Bergmann, K.D., Gómez-Pérez, I., Al Baloushi, B., Boag, T.H., Busch, J.F., Sperling, E.A., Strauss, J.V., 2020. Calibrating the coevolution of Ediacaran life and environment. Proceedings of the National Academy of Sciences of the United States of America 117, 16824–16830. https://doi.org/10.1073/pnas.2002918117

Rooney, A.D., Strauss, J.V., Brandon, A.D., Macdonald, F.A., 2015. A Cryogenian chronology: Two long-lasting synchronous Neoproterozoic glaciations. Geology 43, 459–462. https://doi.org/10.1130/G36511.1

Schiffbauer, J.D., Bykova, N., 2024. Paleontology: Ediacaran ecology drove ocean ventilation. Current Biology 34, R734–R736. https://doi.org/10.1016/j.cub.2024.06.043

Schmitt, R.D.S., Fragoso, R.D.A., Collins, A.S., 2018. Suturing Gondwana in the Cambrian: The Orogenic Events of the Final Amalgamation, in: Siegesmund, S., Basei, M.A.S., Oyhantçabal, P., Oriolo, S. (Eds.), Geology of Southwest Gondwana, Regional Geology Reviews. Springer International Publishing, Cham, pp. 411–432. https://doi.org/10.1007/978-3-319-68920-3_15

Schmoker, J.W., Krystinik, K.B., Halley, R.B., 1985. Selected Characteristics of Limestone and Dolomite Reservoirs in the United States. AAPG Bulletin 69. https://doi.org/10.1306/AD4627F9-16F7-11D7-8645000102C1865D

Schoenborn, W.A., Fedo, C.M., Farmer, G.L., 2012. Provenance of the Neoproterozoic Johnnie Formation and Stirling Quartzite, southeastern California, determined by detrital zircon geochronology and Nd isotope geochemistry. Precambrian Research 206–207, 182–199. https://doi.org/10.1016/j.precamres.2012.02.017

Schrag, D.P., Higgins, John.A., Macdonald, F.A., Johnston, D.T., 2013. Authigenic Carbonate and the History of the Global Carbon Cycle. Science 339, 540–543. https://doi.org/10.1126/science.1229578

Segessenman, D.C., Peters, S.E., 2024. Transgression–regression cycles drive correlations in Ediacaran–Cambrian rock and fossil records. Paleobiology 50, 150–163. https://doi.org/10.1017/pab.2023.31

Segessenman, D.C., Peters, S.E., 2023. Macrostratigraphy of the Ediacaran System in North America, in: Laurentia: Whitmeyer, S.J., Williams, M.L., Kellett, D.A., Tikoff, B. (Eds.), Turning Points in the Evolution of a Continent. Geological Society of America, pp. 399–424. https://doi.org/10.1130/2022.1220(21)

Servais, T., Cascales-Miñana, B., Harper, D.A.T., Lefebvre, B., Munnecke, A., Wang, W., Zhang, Y., 2023. No (Cambrian) explosion and no (Ordovician) event: A single long-term radiation in the early Palaeozoic. Palaeogeography, Palaeoclimatology, Palaeoecology 623, 111592. https://doi.org/10.1016/j.palaeo.2023.111592

Shahkarami, S., Buatois, L.A., Mángano, M.G., Hagadorn, J.W., Almond, J., 2020. The Ediacaran–Cambrian boundary: Evaluating stratigraphic completeness and the Great Unconformity. Precambrian Research 345, 105721. https://doi.org/10.1016/j.precamres.2020.105721

Shi, W., Mills, B.J.W., Algeo, T.J., Poulton, S.W., Newton, R.J., Dodd, M.S., Zhang, Z., Zheng, L., He, T., Hou, M., Li, C., 2023. Heterogeneous sulfide reoxidation buffered oxygen release in the Ediacaran Shuram ocean. Geochimica et Cosmochimica Acta 356, 149–164. https://doi.org/10.1016/j.gca.2023.07.018

Shields, G.A., Mills, B.J.W., Zhu, M., Raub, T.D., Daines, S.J., Lenton, T.M., 2019. Unique Neoproterozoic carbon isotope excursions sustained by coupled evaporite dissolution and pyrite burial. Nature Geoscience 12, 823–827. https://doi.org/10.1038/s41561-019-0434-3

Shore, A.J., Wood, R.A., Butler, I.B., Zhuravlev, A.Yu., McMahon, S., Curtis, A., Bowyer, F.T., 2021. Ediacaran metazoan reveals lophotrochozoan affinity and deepens root of Cambrian Explosion. Science Advances 7, eabf2933. https://doi.org/10.1126/sciadv.abf2933

Siscoe, G.L., Chen, C.-K., 1975. The paleomagnetosphere. Journal of Geophysical Research 80, 4675–4680. https://doi.org/10.1029/JA080i034p04675

Slagter, S., Konhauser, K.O., Briggs, D.E.G., Tarhan, L.G., 2024. Controls on authigenic mineralization in experimental Ediacara-style preservation. Geobiology 22, e12615. https://doi.org/10.1111/gbi.12615

Slagter, S., Tarhan, L.G., Hao, W., Planavsky, N.J., Konhauser, K.O., 2021. Experimental evidence supports early silica cementation of the Ediacara Biota. Geology 49, 51–55. https://doi.org/10.1130/G47919.1

Smith, E.F., Nelson, L.L., O’Connell, N., Eyster, A., Lonsdale, M.C., 2022. The Ediacaran−Cambrian transition in the southern Great Basin, United States. Geological Society of America Bulletin. https://doi.org/10.1130/B36401.1

Smith, E.F., Nelson, L.L., Strange, M.A., Eyster, A.E., Rowland, S.M., Schrag, D.P., Macdonald, F.A., 2016. The end of the Ediacaran: Two new exceptionally preserved body fossil assemblages from Mount Dunfee, Nevada, USA. Geology 44, 911–914. https://doi.org/10.1130/G38157.1

Smith, M.D., Arnott, R.W.C., Ross, G.M., 2014. Physical and geochemical controls on sedimentation along an ancient continental margin: The deep-marine Old Fort Point Formation (Ediacaran), southern Canadian Cordillera. Bulletin of Canadian Petroleum Geology 62, 14–36. https://doi.org/10.2113/gscpgbull.62.1.14

Soukup, M., Beranek, L.P., Lode, S., Goudie, D., Grant, D., 2024. Late Ediacaran to Early Cambrian Breakup Sequences and Establishment of the Eastern Laurentian Passive Margin, Newfoundland, Canada. American Journal of Science 324. https://doi.org/10.2475/001c.93038

Sperling, E.A., Knoll, A.H., Girguis, P.R., 2015. The Ecological Physiology of Earth's Second Oxygen Revolution. Annual Review of Ecology, Evolution, and Systematics 46, 215–235. https://doi.org/10.1146/annurev-ecolsys-110512-135808

Spero, H.J., Bijma, J., Lea, D.W., Bemis, B.E., 1997. Effect of seawater carbonate concentration on foraminiferal carbon and oxygen isotopes. Nature 390, 497–500. https://doi.org/10.1038/37333

Sun, R., Shen, J., Grasby, S.E., Zhang, J., Chen, J., Yang, C., Yin, R., 2022. CO2 buildup drove global warming, the Marinoan deglaciation, and the genesis of the Ediacaran cap carbonates. Precambrian Research 383, 106891. https://doi.org/10.1016/j.precamres.2022.106891

Swart, P.K., 2015. The geochemistry of carbonate diagenesis: The past, present and future. Sedimentology 62, 1233–1304. https://doi.org/10.1111/sed.12205

Tan, Z., Luo, J., Xu, X., Jia, W., Li, J., Chen, L., 2024. New Re–Os Geochronological Data from the Upper Doushantuo Formation: Age Constraint on the Shuram Excursion and Implication for the Ediacaran Fluctuated Continental Weathering. ACS Omega 9, 49121–49131. https://doi.org/10.1021/acsomega.4c05072

Tarhan, L.G., Hood, A. v.S., Droser, M.L., Gehling, J.G., Briggs, D.E.G., 2016. Exceptional preservation of soft-bodied Ediacara Biota promoted by silica-rich oceans. Geology 44, 951–954. https://doi.org/10.1130/G38542.1

Tasistro-Hart, A.R., Macdonald, F.A., 2023. Phanerozoic flooding of North America and the Great Unconformity. Proceedings of the National Academy of Sciences of the United States of America 120, e2309084120. https://doi.org/10.1073/pnas.2309084120

Thomas, W.A., 1991. The Appalachian-Ouachita rifted margin of southeastern North America. Geological Society of America Bulletin 103, 415–431. https://doi.org/10.1130/0016-7606(1991)103<0415:TAORMO>2.3.CO;2

Tian, X., Buck, W.R., 2022. Intrusions induce global warming before continental flood basalt volcanism. Nature Geoscience 15, 417–422. https://doi.org/10.1038/s41561-022-00939-w

Tomkins, A.G., Martin, E.L., Cawood, P.A., 2024. Evidence suggesting that earth had a ring in the Ordovician. Earth and Planetary Science Letters 646, 118991. https://doi.org/10.1016/j.epsl.2024.118991

Urey, H.C., 1952. On the Early Chemical History of the Earth and the Origin of Life. Proceedings of the National Academy of Sciences of the United States of America 38, 351–363. https://doi.org/10.1073/pnas.38.4.351

Valentine, J.W., Moores, E.M., 1970. Plate-tectonic Regulation of Faunal Diversity and Sea Level: a Model. Nature 228, 657–659. https://doi.org/10.1038/228657a0

Van Staal, C.R., Zagorevski, A., 2023. Paleozoic tectonic evolution of the rifted margins of Laurentia, in: Whitmeyer, S.J., Williams, M.L., Kellett, D.A., Tikoff, B. (Eds.), Laurentia: Turning Points in the Evolution of a Continent. Geological Society of America, pp. 487–503. https://doi.org/10.1130/2022.1220(24)

Wala, V.T., Ziemniak, G., Majka, J., Faehnrich, K., McClelland, W.C., Meyer, E.E., Manecki, M., Bazarnik, J., Strauss, J.V., 2021. Neoproterozoic stratigraphy of the Southwestern Basement Province, Svalbard (Norway): Constraints on the Proterozoic-Paleozoic evolution of the North Atlantic-Arctic Caledonides. Precambrian Research 358, 106138. https://doi.org/10.1016/j.precamres.2021.106138

Waldron, J.W.F., Schofield, D.I., Murphy, J.B., 2019. Diachronous Paleozoic accretion of peri-Gondwanan terranes at the Laurentian margin. Geological Society of London Special Publications 470, 289–310. https://doi.org/10.1144/SP470.11

Walton, C.R., Hao, J., Huang, F., Jenner, F.E., Williams, H., Zerkle, A.L., Lipp, A., Hazen, R.M., Peters, S.E., Shorttle, O., 2023. Evolution of the crustal phosphorus reservoir. Science Advances 9, eade6923. https://doi.org/10.1126/sciadv.ade6923

Wang, H., Peng, Y., Li, C., Cao, X., Cheng, M., Bao, H., 2023. Sulfate triple-oxygen-isotope evidence confirming oceanic oxygenation 570 million years ago. Nature Communications 14, 4315. https://doi.org/10.1038/s41467-023-39962-9

Wang, R., Shen, B., Lang, X., Wen, B., Mitchell, R.N., Ma, H., Yin, Z., Peng, Y., Liu, Y., Zhou, C., 2023a. A Great late Ediacaran ice age. National Science Review 10, nwad117. https://doi.org/10.1093/nsr/nwad117

Wang, R., Xing, C., Wen, B., Wang, X., Liu, K., Huang, T., Zhou, C., Shen, B., 2023b. The origin of cap carbonate after the Ediacaran glaciations. Global and Planetary Change 226, 104141. https://doi.org/10.1016/j.gloplacha.2023.104141

Wang, R., Yin, Z., Shen, B., 2023c. A late Ediacaran ice age: The key node in the Earth system evolution. Earth-Science Reviews 247, 104610. https://doi.org/10.1016/j.earscirev.2023.104610

Wang, W., Li, C., Dodd, M.S., Algeo, T.J., Zhang, Z., Cheng, M., Hou, M., 2023. A DOM regulation model for dolomite versus calcite precipitation in the Ediacaran ocean:

Implications for the “dolomite problem.” Precambrian Research 385, 106947. https://doi.org/10.1016/j.precamres.2022.106947

Wang, X., Zhang, X., Zhang, Y., Cui, L., Li, L., 2021. New materials reveal Shaanxilithes as a Cloudina-like organism of the late Ediacaran. Precambrian Research 362, 106277. https://doi.org/10.1016/j.precamres.2021.106277

Wei, G.-Y., Zhao, M., Sperling, E.A., Gaines, R.R., Kalderon-Asael, B., Shen, J., Li, C., Zhang, F., Li, G., Zhou, C., Cai, C., Chen, D., Xiao, K.-Q., Jiang, L., Ling, H.-F., Planavsky, N.J., Tarhan, L.G., 2024. Lithium isotopic constraints on the evolution of continental clay mineral factory and marine oxygenation in the earliest Paleozoic Era. Science Advances 10, eadk2152. https://doi.org/10.1126/sciadv.adk2152

Weil, A.B., Yonkee, A., 2023. The Laramide orogeny: Current understanding of the structural style, timing, and spatial distribution of the classic foreland thick-skinned tectonic system, in: Whitmeyer, S.J., Williams, M.L., Kellett, D.A., Tikoff, B. (Eds.), Laurentia: Turning Points in the Evolution of a Continent. Geological Society of America, pp. 707–771. https://doi.org/10.1130/2022.1220(33)

Wilkinson, B., Walker, J.G.G., 1989. Phanerozoic Cycling of Sedimentary Carbonate. American Journal of Science 289, 525–548. https://doi.org/10.2475/ajs.289.4.525

Williams, G.E., Schmidt, P.W., 2021. Dating the Acraman asteroid impact, South Australia: the case for deep drilling the ‘hot shock’ zone of the central uplift. Australian Journal of Earth Sciences 68, 355–367. https://doi.org/10.1080/08120099.2020.1808066

Williams, H., King, A.F., 1979. Trepassey Map Area, Newfoundland. Geological Survey of Canada Memoir 389, 24 p.

Willman, S., Peel, J.S., Ineson, J.R., Schovsbo, N.H., Rugen, E.J., Frei, R., 2020. Ediacaran Doushantuo-type biota discovered in Laurentia. Nature Communications Biology 3, 647. https://doi.org/10.1038/s42003-020-01381-7

Wilson, J.T., 1966. Did the Atlantic Close and then Re-open? Nature 211, 676–681. https://doi.org/10.1038/211676a0

Wong Hearing, T.W., Pohl, A., Williams, M., Donnadieu, Y., Harvey, T.H.P., Scotese, C.R., Sepulchre, P., Franc, A., Vandenbroucke, T.R.A., 2021. Quantitative comparison of geological data and model simulations constrains early Cambrian geography and climate. Nature Communications 12, 3868. https://doi.org/10.1038/s41467-021-24141-5

Wood, R., Liu, A.G., Bowyer, F., Wilby, P.R., Dunn, F.S., Kenchington, C.G., Cuthill, J.F.H., Mitchell, E.G., Penny, A., 2019. Integrated records of environmental change and evolution challenge the Cambrian Explosion. Nat Ecology & Evolution 3, 528–538. https://doi.org/10.1038/s41559-019-0821-6

Wu, C., Hua, H., Zeng, Z., Zheng, Y., Yang, D., Jiao, R., 2024. An Ediacaran glacial deposit in southern margin of the North China Craton: The Luoquan Formation—sedimentology, geochronology and provenance. Geological Journal 59, 2336–2363. https://doi.org/10.1002/gj.5022

Xiao, S.H., Narbonne, G.M., 2020. The Ediacaran Period, in: Gradstein, F.M., Ogg, J.G., Schmitz, M.D., Ogg, G.M. (Eds.), Geologic Time Scale 2020. Elsevier, pp. 521–561. https://doi.org/10.1016/B978-0-12-824360-2.00018-8

Xu, D., Wang, X., Shi, X., Peng, Y., Stüeken, E.E., 2021. Feedback Between Carbon and Nitrogen Cycles During the Ediacaran Shuram Excursion. Frontiers in Earth Science 9, 678149. https://doi.org/10.3389/feart.2021.678149

Yang, C., Rooney, A.D., Condon, D.J., Li, X.-H., Grazhdankin, D.V., Bowyer, F.T., Hu, C., Macdonald, F.A., Zhu, M., 2021. The tempo of Ediacaran evolution. Science Advances 7, eabi9643. https://doi.org/10.1126/sciadv.abi9643

Ye, Y., Frings, P.J., Von Blanckenburg, F., Feng, Q., 2021. Silicon isotopes reveal a decline in oceanic dissolved silicon driven by biosilicification: A prerequisite for the Cambrian Explosion? Earth and Planetary Science Letters 566, 116959. https://doi.org/10.1016/j.epsl.2021.116959

Youbi, N., Ernst, R.E., Mitchell, R.N., Boumehdi, M.A., El Moume, W., Lahna, A.A., Bensalah, M.K., Söderlund, U., Doblas, M., Tassinari, C.C.G., 2021. Preliminary Appraisal of a Correlation Between Glaciations and Large Igneous Provinces Over the Past 720 Million Years, in: Ernst, R.E., Dickson, A.J., Bekker, A. (Eds.), Geophysical Monograph Series. Wiley, pp. 169–190. https://doi.org/10.1002/9781119507444.ch8

Zaffos, A., Finnegan, S., Peters, S.E., 2017. Plate tectonic regulation of global marine animal diversity. Proceedings of the National Academy of Sciences of the United States of America 114, 5653–5658. https://doi.org/10.1073/pnas.1702297114

Zhang, F., Xiao, S., Romaniello, S.J., Hardisty, D., Li, C., Melezhik, V., Pokrovsky, B., Cheng, M., Shi, W., Lenton, T.M., Anbar, A.D., 2019. Global marine redox changes drove the rise and fall of the Ediacara biota. Geobiology 17, 594–610. https://doi.org/10.1111/gbi.12359

Zhang, Y., Zhu, G., Li, X., Ai, Y., Duan, P., Li, M., Liu, J., 2024. Chemical–to–reverse weathering triggered a pronounced positive carbon isotope excursion in a forced regressive to transgressive dolostone succession during the terminal Ediacaran glaciation.

Global and Planetary Change 240, 104521. https://doi.org/10.1016/j.gloplacha.2024.104521

Zheng, K., Li, S., Gao, Y., Meng, W., Cheng, H., 2024. Advances in Reverse Weathering and Its Role in Clay Mineral Formation and the Carbon Dioxide Cycle. ACS Earth and Space Chemistry 8, 1680–1689. https://doi.org/10.1021/acsearthspacechem.4c00105

Figure and Table Captions

Figure 1 – Map of North America, Greenland (insert), and Svalbard (insert) with plotted areas of Ediacaran age stratigraphic columns colored by whether they contain carbonate or not (blue and gray, respectively) with locations of measured $\delta^{13}C$ and $\delta^{18}O$ compiled for this study (orange diamonds). Locations of geochemical measurements randomly jittered for visibility in high-density localities. Plotted Ediacaran stratigraphic data is from Segessenman and Peters, 2023.

Figure 2 – Time series of Ediacaran preserved sedimentary rock quantities and compiled carbonate $\delta^{13}C$ and $\delta^{18}O$ measurements anchored to rock quantity using a modified age model from Segessenman and Peters, 2023 with potentially relevant significant Ediacaran events highlighted. A full list of event timings and references can be found in Table 2. Three myr smoothing was applied to all rock quantity curves. Volume flux is reported in units of km^3/myr and area is reported in units of km^2. Carbonate quantities are split into three depositional environmental categories of nearshore, outer shelf, and slope/basin settings, in addition in an inferred marine category for carbonates with no clear environmental interpretation. A full list of carbonate rock units and their environmental interpretations from the published literature can be found in Table 1. A) volume flux, separated by depositional environment, and overlaid with raw

$\delta^{13}C$ values; B) area of Ediacaran carbonates separated by depositional environment categories; C) volume flux of total marine siliciclastic and carbonate sedimentary rocks and counts of the number of sedimentary rock units through time; and D) area of total marine siliciclastic and carbonate sedimentary rocks and proportion of sedimentary rock units that have carbonate present.

Figure 3 – Time series of Ediacaran carbonate raw carbonate isotopic values and rock quantities split by phase (dolomite, calcite, and marble/unknown) and depositional environmental category (nearshore, outer shelf, and slope/basin) with potentially relevant significant Ediacaran events highlighted. A full list of event timings and references can be found in Table 2. Three myr smoothing was applied to all rock quantity curves. Volume flux is reported in units of km^3/myr and area is reported in units of km^2. A) time series of raw carbonate $\delta^{13}C$ values colored by phase; B) volume flux of limestone; C) volume flux of dolostone; D) area of limestone; E) area of dolostone.

Figure 4 – Time series of carbonate $\delta^{13}C$ averaged by locality, phase, and depositional environment category, and 5 myr moving window Spearman's ρ correlations between $\delta^{13}C$ and $\delta^{18}O$ values with potentially relevant significant Ediacaran events highlighted. A full list of event timings and references can be found in Table 2. Three myr smoothing was applied to all time series except that of locality. All averages were calculated with 3 myr moving window averages in which each relevant locality was averaged first, then the average of the locality averages was calculated to avoid biasing averages towards localities with greater sampling density. Bootstrap resampled error bars and confidence intervals were calculated and plotted for each time series.

A) $\delta^{13}C$ values averaged across localities; B) $\delta^{13}C$ values averaged by phase (calcite and dolomite); C) $\delta^{13}C$ values averaged by depositional environment category (nearshore, outer shelf, and slope/basin); and D) Spearman's ρ correlations between $\delta^{13}C$ and $\delta^{18}O$ values.

Figure 5 – Time series of carbonate raw $\delta^{18}O$ and averages separated by locality, phase, and depositional environment category with potentially relevant significant Ediacaran events highlighted. A full list of event timings and references can be found in Table 2. Three myr smoothing was applied to environmental and phase averages. All averages were calculated with 3 myr moving window averages in which each relevant locality was averaged first, then the average of the locality averages was calculated to avoid biasing averages towards localities with greater sampling density. Bootstrap resampled error bars and confidence intervals were calculated and plotted for each time series except the raw values plot. A) raw $\delta^{18}O$ values colored by depositional environment category (nearshore, outer shelf, and slope/basin); B) $\delta^{18}O$ values averaged by depositional environment category; C) $\delta^{18}O$ values averaged by locality; and D) $\delta^{18}O$ values averaged by phase (calcite and dolomite).

Table 1 – North American Ediacaran carbonate bearing unit names, their locality, their interpreted relative age, assigned depositional environment category for this study, the main interpretive statement from publications that supports our environmental category assignment, and the primary reference this evidence comes from.

Table 2 – Significant Ediacaran events highlighted on Figures 2-5, the timings/age ranges used for this study, relevant notes on interpretations of these events, and the publications that evidence and timings of the events can be found.

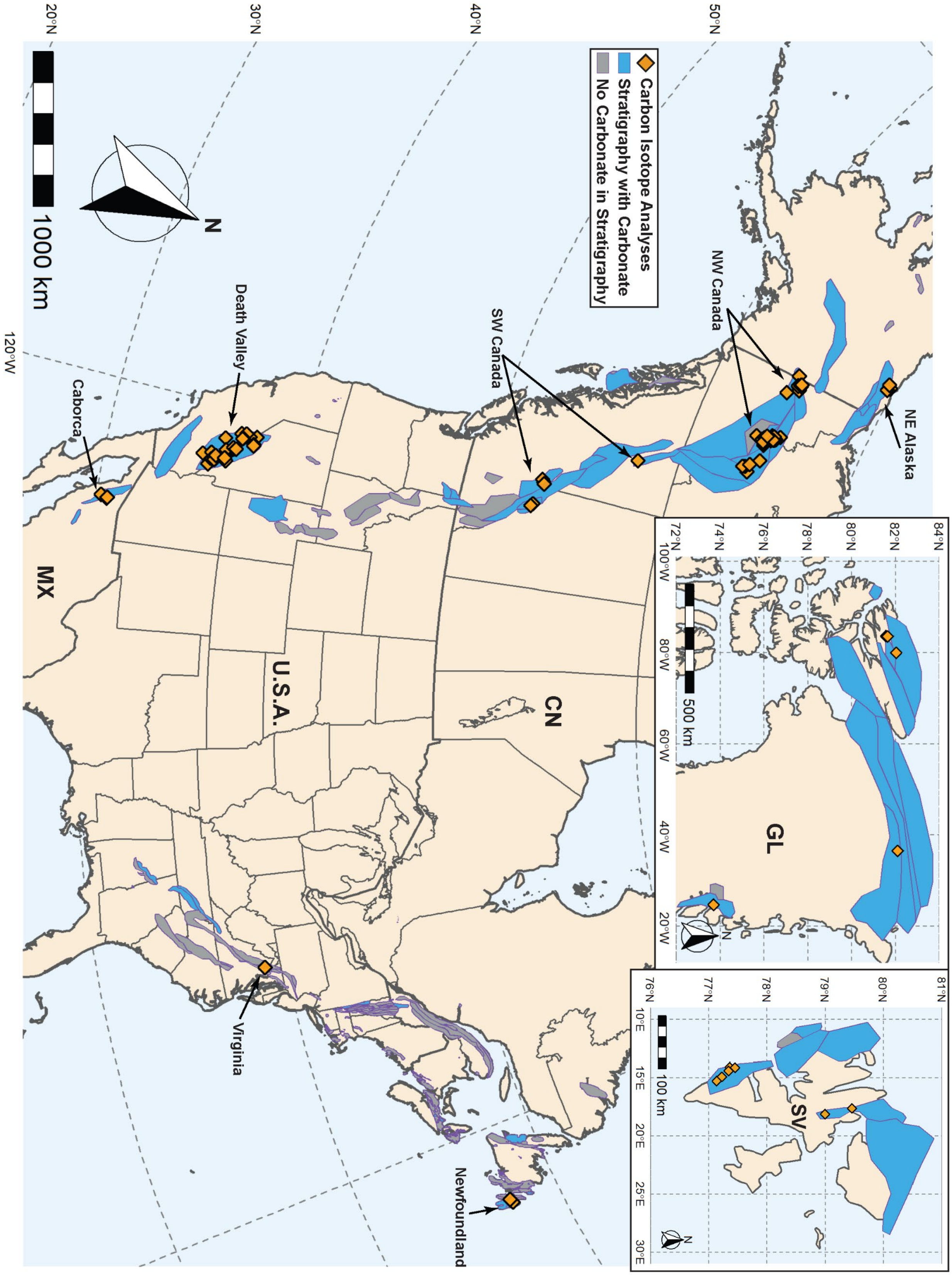
Carbon Isotope Analyses
Stratigraphy with Carbonate
No Carbonate in Stratigraphy
N
1000 km
20°N
30°N
40°N
50°N
120°W
NE Alaska
NW Canada
SW Canada
Death Valley
Caborca
Virginia
Newfoundland
CN
U.S.A.
MX
GL
72°N
74°N
76°N
78°N
80°N
82°N
84°N
100°W
80°W
60°W
40°W
20°W
500 km
SV
76°N
77°N
78°N
79°N
80°N
81°N
10°E
15°E
20°E
25°E
30°E
100 km

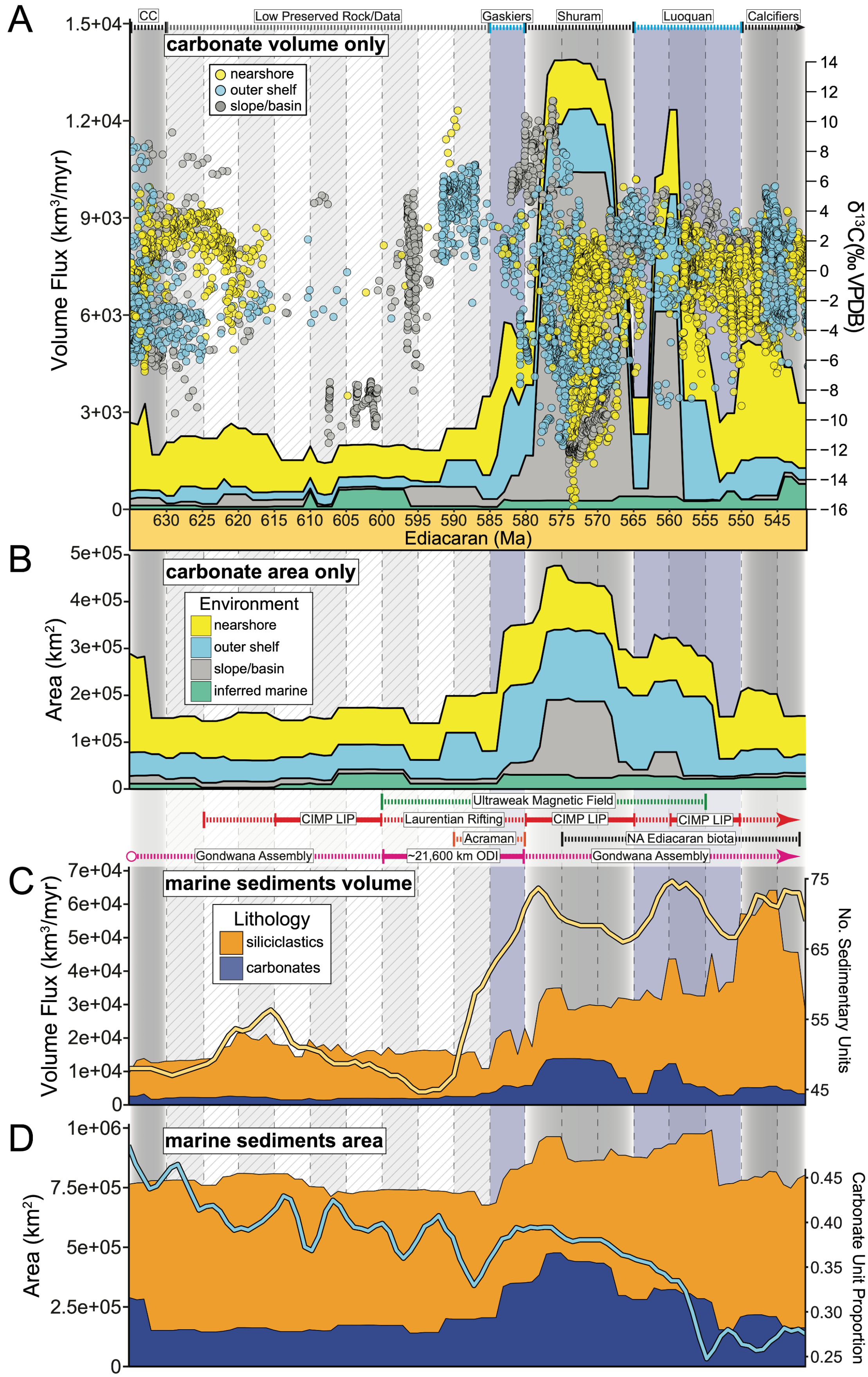

A
carbonate volume only
nearshore
outer shelf
slope/basin
CC
Low Preserved Rock/Data
Gaskiers
Shuram
Luoquan
Calcifiers
Volume Flux (km³/myr)
δ13C(‰ VPDB)
Ediacaran (Ma)
B
carbonate area only
Environment
nearshore
outer shelf
slope/basin
inferred marine
Area (km²)
Ultraweak Magnetic Field
CIMP LIP
Laurentian Rifting
CIMP LIP
CIMP LIP
Acraman
NA Ediacaran biota
Gondwana Assembly
~21,600 km ODI
Gondwana Assembly
C
marine sediments volume
Lithology
siliciclastics
carbonates
Volume Flux (km³/myr)
No. Sedimentary Units
D
marine sediments area
Area (km²)
Carbonate Unit Proportion

1508

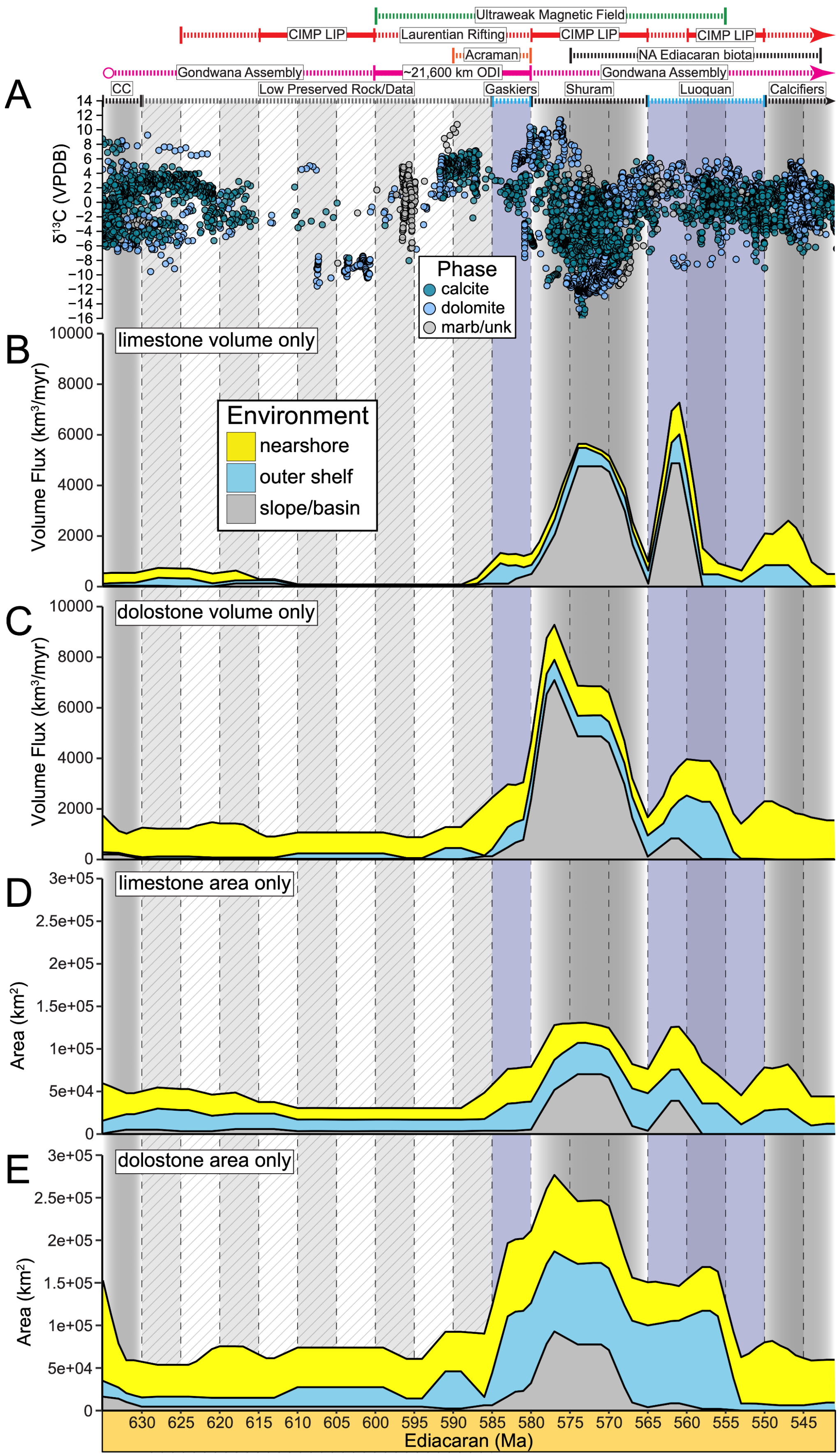
Ultraweak Magnetic Field
CIMP LIP
Laurentian Rifting
CIMP LIP
CIMP LIP
Acraman
NA Ediacaran biota
Gondwana Assembly
~21,600 km ODI
Gondwana Assembly
CC
Low Preserved Rock/Data
Gaskiers
Shuram
Luoquan
Calcifiers
A
δ13C (VPDB)
Phase
calcite
dolomite
marb/unk
B
limestone volume only
Volume Flux (km3/myr)
Environment
nearshore
outer shelf
slope/basin
C
dolostone volume only
Volume Flux (km3/myr)
D
limestone area only
Area (km2)
E
dolostone area only
Area (km2)
Ediacaran (Ma)

1509

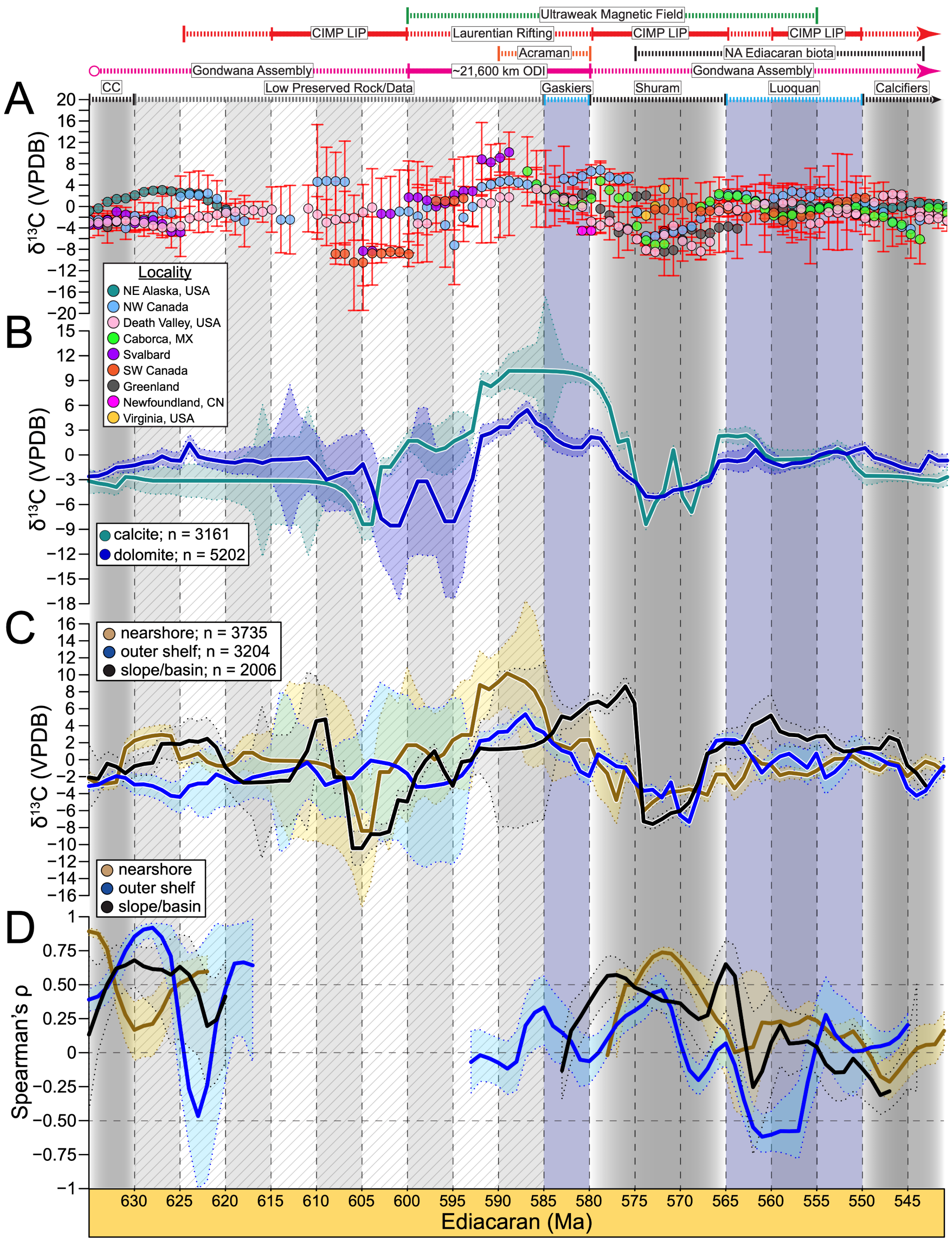
Ultraweak Magnetic Field
CIMP LIP
Laurentian Rifting
CIMP LIP
CIMP LIP
Acraman
NA Ediacaran biota
Gondwana Assembly
~21,600 km ODI
Gondwana Assembly
CC
Low Preserved Rock/Data
Gaskiers
Shuram
Luoquan
Calcifiers
A
B
C
D
δ13C (VPDB)
Locality
NE Alaska, USA
NW Canada
Death Valley, USA
Caborca, MX
Svalbard
SW Canada
Greenland
Newfoundland, CN
Virginia, USA
calcite; n = 3161
dolomite; n = 5202
nearshore; n = 3735
outer shelf; n = 3204
slope/basin; n = 2006
nearshore
outer shelf
slope/basin
Spearman's ρ
Ediacaran (Ma)

1510

1511

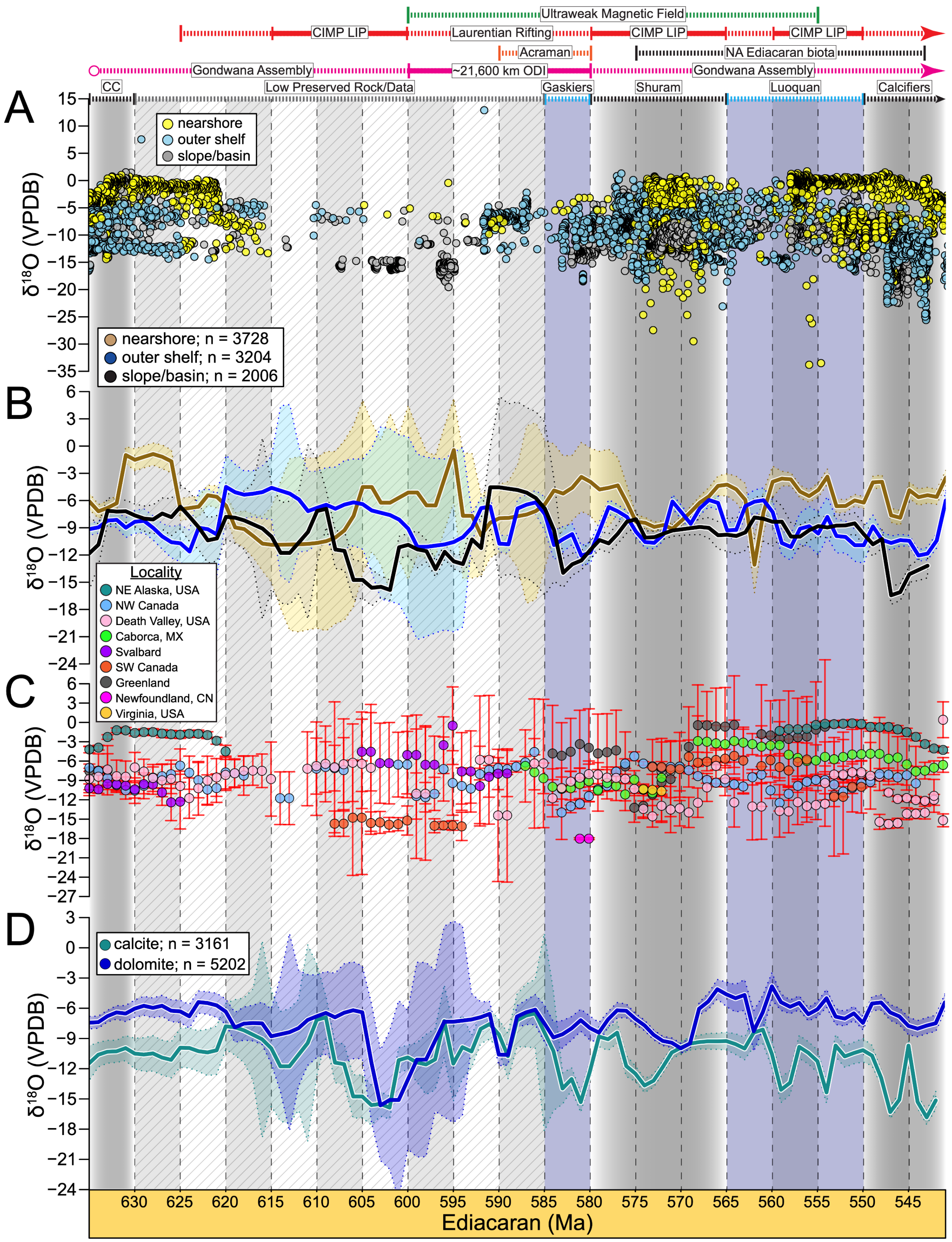
Ultraweak Magnetic Field
CIMP LIP
Laurentian Rifting
CIMP LIP
CIMP LIP
Acraman
NA Ediacaran biota
Gondwana Assembly
~21,600 km ODI
Gondwana Assembly
CC
Low Preserved Rock/Data
Gaskiers
Shuram
Luoquan
Calcifiers
A
nearshore
outer shelf
slope/basin
nearshore; n = 3728
outer shelf; n = 3204
slope/basin; n = 2006
B
Locality
NE Alaska, USA
NW Canada
Death Valley, USA
Caborca, MX
Svalbard
SW Canada
Greenland
Newfoundland, CN
Virginia, USA
C
D
calcite; n = 3161
dolomite; n = 5202
δ18O (VPDB)
Ediacaran (Ma)

1512

1513

Carbonate Bearing Unit	Region	Interpreted Age	Environment Category	Main Interpretive Statement from Literature	Reference
Canyon Fm	Greenland	earliest Ediacaran	nearshore	forms the transgressive tract (cap dolostone) of the depositional sequence. The highstand tract culminates with shallow-water dolarenite	Hoffman et al., 2012
Portfjeld Fm	Greenland	mid-late Ediacaran	nearshore	Typical facies include hummocky cross-stratified intraclast-rich grainstones and cherty dark dolostones of the mid- and outer ramp, and ooid–pisoid grainstones and varied microbial facies of the inner ramp	Willman et al., 2020
Katakturuk Dolomite K2	NE Alaska	earliest Ediacaran	slope/basin	Lower slope limestone rhythmites, turbidites, debris flows and shale	Macdonald et al., 2009
Katakturuk Dolomite K2	NE Alaska	earliest Ediacaran	nearshore	Back reef and ramp dolo-grainstone; Shoal complex dolo-microbialite	Macdonald et al., 2009
Katakturuk Dolomite K3	NE Alaska	early Ediacaran	nearshore	Back reef and ramp dolo-grainstone; Shoal complex dolo-microbialite	Macdonald et al., 2009
Katakturuk Dolomite K3	NE Alaska	early Ediacaran	slope/basin	Lower slope limestone rhythmites, turbidites, debris flows and shale	Macdonald et al., 2009
Katakturuk Dolomite K4	NE Alaska	latest Ediacaran	nearshore	Back reef and ramp dolo-grainstone	Macdonald et al., 2009
Algae Fm	NW Canada	late Ediacaran	slope/basin	likely accumulated through a combination of hemipelagic carbonate sedimentation, sediment-gravity flows, and traction sedimentation as indicated by the sedimentary structures and depositional features	Moynihan et al., 2019
Blueflower Fm	NW Canada	late Ediacaran	outer shelf	uppermost strata of the Blueflower Formation shoal gradationally into medium-bedded sandstone with hummocky cross stratification; transition from shelf to shoreface	Macdonald et al., 2013
Blueflower Fm	NW Canada	late Ediacaran	slope/basin	mostly dominated by slope sedimentation. This is supported by the dominance of siliciclastic and mixed clastic-carbonate strata characterized by turbidites, slump folds, and soft-sediment deformation, and debris flow horizons	Moynihan et al., 2019
Cliff Creek Fm	NW Canada	earliest Ediacaran	outer shelf	Fig. 12 of Busch et al., 2021	Busch et al., 2021
Fireweed Mbr	NW Canada	late Ediacaran	outer shelf	Fig. 12 of Busch et al., 2021	Busch et al., 2021
Gametrail Fm	NW Canada	late Ediacaran	slope/basin	The type Gametrail Formation is ~200 m thick and consists predominantly of thin-bedded limestone interbedded with massive carbonate debris flows and olistoliths	Macdonald et al., 2013
Gametrail Fm	NW Canada	late Ediacaran	nearshore	inner ramp/reef complex/shoal complex	Busch et al., 2022
Gladman Mbr	NW Canada	mid-late Ediacaran	outer shelf	Fig. 12 of Busch et al., 2021	Busch et al., 2021
Hayhook Fm	NW Canada	earliest Ediacaran	nearshore	interpreted correlative strata in the shallow-water Hayhook Formation in the Mackenzie Mountains	Cochrane et al., 2019
Last Chance Mbr	NW Canada	late Ediacaran	outer shelf	Fig. 12 of Busch et al., 2021	Busch et al., 2021
Nadaleen Fm	NW Canada	upper Ediacaran	slope/basin	exhibits characteristic features of slope to basin floor sedimentation through a combination of suspension deposition and submarine sediment gravity flows	Moynihan et al., 2019
Ravensthroat Fm	NW Canada	earliest Ediacaran	outer shelf	These strata most likely record hemipelagic carbonate sedimentation in a slope or outer-shelf setting	Moynihan et al., 2019
Risky Fm	NW Canada	latest Ediacaran	nearshore	nearshore facies characterized by trough cross-bedded sandstone, stromatolites, oolitic grainstone, and paleokarst surfaces within the Risky Formation	Macdonald et al., 2013
Sheepbed Carbonate	NW Canada	early Ediacaran	outer shelf	Exposures in the Wernecke Mountains clearly demonstrate that the Sheepbed carbonate is the HST deposit of Sequence 1	Macdonald et al., 2013
Sheepbed Fm	NW Canada	early Ediacaran	slope/basin	consists of >700m of siliciclastics deposited in a proximal to distal slope environment	Rooney et al., 2015
Upper Rackla Gp	NW Canada	late Ediacaran	outer shelf	marine shelf	Macdonald et al., 2013
Caborca Fm	NW Mexico	early Ediacaran	outer shelf	represent predominantly shallow marine carbonate and siliciclastic depositional environments generally no deeper than continental shelf depths	Loyd et al., 2012
Clemente Fm	NW Mexico	mid-late Ediacaran	outer shelf	represent predominantly shallow marine carbonate and siliciclastic depositional environments generally no deeper than continental shelf depths	Loyd et al., 2012
El Arpa Fm	NW Mexico	early Ediacaran	outer shelf	represent predominantly shallow marine carbonate and siliciclastic depositional environments generally no deeper than continental shelf depths	Loyd et al., 2012
Gamuza Fm	NW Mexico	late Ediacaran	outer shelf	represent predominantly shallow marine carbonate and siliciclastic depositional environments generally no deeper than continental shelf depths	Loyd et al., 2012
La Cienega	NW Mexico	latest Ediacaran	outer shelf	represent predominantly shallow marine carbonate and siliciclastic depositional environments generally no deeper than continental shelf depths	Loyd et al., 2012
La Cienega	NW Mexico	latest Ediacaran	nearshore	shoreface to peritidal	Hodgin et al., 2021
Paplote Fm	NW Mexico	late Ediacaran	outer shelf	represent predominantly shallow marine carbonate and siliciclastic depositional environments generally no deeper than continental shelf depths	Loyd et al., 2012
Tecolote Fm	NW Mexico	late Ediacaran	outer shelf	represent predominantly shallow marine carbonate and siliciclastic depositional environments generally no deeper than continental shelf depths	Loyd et al., 2012
Harbour Main Fm	SE Canada	mid-late Ediacaran	outer shelf	was probably inorganically precipitated and deposited well below the photic zone; lacks slope/basin structures	Myrow and Kaufman, 1999
Fauquier Fm	SE USA	late Ediacaran	outer shelf	suggesting a shallower proximal marine to fluvial setting	Hebert et al., 2010
Dracoisen Cap Carbonate	Svalbard	earliest Ediacaran	nearshore	forms the transgressive base of the Dracoisen cap carbonate sequence. The 3–15-m-thick, yellow to buff-weathering cap dolostone contains megaripples and peloids	Halverson et al., 2005
Dracoisen Fm	Svalbard	early Ediacaran	nearshore	Above this level, the remainder of the Dracoisen consists mostly of mudcracked and ripple cross-laminated red and green siltstones	Halverson et al., 2004
Hoferpynten Fm	Svalbard	earliest Ediacaran	outer shelf	finely laminated dolostone units that host distinct sedimentary structures, such as sheet crack cements, m-scale trochoidal bedforms, and finely laminated peloidal dolograinstone	Wala et al., 2021
Slettfjelldalen Fm	Svalbard	earliest Ediacaran	outer shelf	finely laminated dolostone units that host distinct sedimentary structures, such as sheet crack cements, m-scale trochoidal bedforms, and finely laminated peloidal dolograinstone	Wala et al., 2021
Isaac Fm	SW Canada	early-late Ediacaran	slope/basin	mixed carbonate-siliciclastic base-of-slope succession	Cochrane et al., 2019
Matulka Gp	SW Canada	late Ediacaran	nearshore	A high-energy subtidal depositional setting associated with tidal sand bars and/or a migrating barrier complex	Eyster et al., 2018
Old Fort Point Fm	SW Canada	early Ediacaran	slope/basin	variety of deep-marine processes in slope to basin-floor settings	Smith et al., 2014
Dunfee Mbr	SW USA	late Ediacaran	nearshore	shallow marine to shoreface	Corsetti and Kaufman, 1994
Dunfee Mbr	SW USA	late Ediacaran	outer shelf	consists of mixed carbonate-siliciclastic deposits representing slope to shallow subtidal settings	Smith et al., 2016
Dunfee Mbr	SW USA	late Ediacaran	slope/basin	consists of mixed carbonate-siliciclastic deposits representing slope to shallow subtidal settings	Smith et al., 2016
Esmeralda Mbr	SW USA	late Ediacaran	nearshore	green shoreface sandstone with mud cracks, interference ripples, and bed-planar trace fossils	Smith et al., 2016
Johnnie Fm	SW USA	early-late Ediacaran	nearshore	contains mixed siliciclastic-carbonate lithofacies interpreted to represent shallow-marine deposition with minor fluvial influence	Corsetti and Kaufman, 2003
Johnnie Fm	SW USA	mid-late Ediacaran	outer shelf	Proximal to distal reconstruction of Johnnie Fm from oolite to base of the Stirling	Bergmann et al., 2011
Mahogany Flats Mbr	SW USA	early Ediacaran	nearshore	relatively uniform basinwide subsidence occurred during Mahogany Flats time, which was marked by deposition of stromatolitic and shallow-water dolostones	Petterson et al., 2011
Noonday Dolomite	SW USA	early Ediacaran	outer shelf	interpreted to contain large domes (up to 200 m in diameter) interpreted as megastromatolites that approach the shelf margin	Corestti and Kaufman, 2003
Radcliff Mbr	SW USA	earliest Ediacaran	nearshore	tidal marine; limestone rhythmites	Petterson et al., 2011
Radcliff Mbr	SW USA	earliest Ediacaran	outer shelf	the distally steepened shelf succession, originally designated as the Ibex Formation Limestone and Shaley Limestone members	Creveling et al., 2016
Reed Dolomite	SW USA	late Ediacaran	outer shelf	thickly bedded with no shallow/high-energy structures reported	Smith et al., 2023
Sentinel Peak Mbr	SW USA	earliest Ediacaran	slope/basin	slope; sheet cracks and tubestone	Petterson et al., 2011
Sitrling Quartzite	SW USA	late Ediacaran	nearshore	middle member of intertidal marine origin composed of dark gray platy siltstone, shale, and variable amounts of dolomite	Schoenborn et al., 2012
Wood Canyon	SW USA	latest Ediacaran	nearshore	The lower and middle members of the Wood Canyon Formation record a shallow marine-continental braid-plain transition	Hagadorn and Waggoner, 2000
Wyman Fm	SW USA	early-late Ediacaran	outer shelf	The section primarily represents shallow marine deposition; has trace fossils such Helminthoidichnites present	Corsetti and Hagadorn, 2000
Yelverton Fm	N Canada	latest Ediacaran	outer shelf	shallow-marine carbonates (via Trettin, 1998)	Faehnrich et al., 2023

Event	Timing/Age Range	Notes	Reference(s)
Laurentian Rifting	Late Tonian - Early Cambrian	North America western and eastern margins have overlapping but separate rift timings	Macdonald et al., 2023 and references therein
Central Iapetan Magmatic Province (CIMP) LIP	615-600 Ma; 580-565; 560-550 Ma	see supplement of Condie et al., 2021 for detailed timings and evidence	Condie et al., 2021; Ernst et al., 2021; Robert et al., 2021; Youbi et al., 2021; Macdonald et al., 2023; Soukup et al., 2024
Ultraweak Magnetic Field	600-555 Ma	see highlighted UL-TAFI in Fig. 3 of Huang et al., 2024	Domeier et al., 2023; Huang et al., 2024
Acraman Impact Crater	590-580 Ma	age based on Rb-Sr shale dating and chemmostratigraphy	Williams and Schmidt, 2021
Gaskiers Glaciation	?585-580 Ma	Pu et al., 2016 tightly constrained Gaskiers Fm glacial evidence, but Fitzgerald et al., 2024 discovered further evidence of glacial activity in underlying Mall Bay Fm.	Pu et al., 2016; Fitzgerald et al., 2024
Shuram-Wonoka Excursion	580-565 Ma	Timings from Rooney et al., 2020 and Cantine et al., 2024 provide tighter constraints assuming synchroneity; in this study our timing is also based on our age model	Rooney et al., 2020; Cantine et al., 2024
North American Ediacaran Biota	~575-539 Ma	Age range is a composite of many different fossil lineages and covers Avalon, White Sea, and Nama assemblages; youngest NA Ediacaran biota from SE USA	Xiao and Narbonne, 2020 and references therein
Gondwana Assembly	Early Ediacaran - Early Paleozoic	large number of orogenies associated with prolonged Gondwana supercontinent formation	Oriolo et al., 2017; Condie et al., 2021
Major Orogenic Deformation Initiation (MODI)	600-580 Ma	This refers to an anomalously increased (compared to preceding and following 10s of millions of years) length of orogenic fronts in which deformation initiates	Condie et al., 2021 and references therein
Luoquan Glaciation	~565-550 Ma	Hankalchough and Luoquan formations both have proposed late Ediacaran glacial influence, we used Luoquan glaciation here due to Wu et al., 2024's tighter constraints	Wang et al., 2023a; Wang et al., 2023b; Wu et al., 2024
Advent of Calcifying Metazoans	~551-550 Ma	Age range given is for advent of metazoan (*Cloudina*) biomineralization, not the full duration of the earliest biomineralizers	Xiao and Narbonne, 2020; Bowyer et al., 2023